

ARL-TN-1014 • APR 2020



# Low-Noise Amplifiers (LNAs) and Power Amplifiers (PAs) for Next-Generation S- and X-Band Radars' Testing

by John E Penn

Approved for public release; distribution is unlimited.

## **NOTICES**

### **Disclaimers**

The findings in this report are not to be construed as an official Department of the Army position unless so designated by other authorized documents.

Citation of manufacturer's or trade names does not constitute an official endorsement or approval of the use thereof.

Destroy this report when it is no longer needed. Do not return it to the originator.



# Low-Noise Amplifiers (LNAs) and Power Amplifiers (PAs) for Next-Generation S- and X-Band Radars' Testing

**John E Penn**

*Sensors and Electron Devices Directorate, CCDC Army Research Laboratory*

**REPORT DOCUMENTATION PAGE**

*Form Approved  
OMB No. 0704-0188*

Public reporting burden for this collection of information is estimated to average 1 hour per response, including the time for reviewing instructions, searching existing data sources, gathering and maintaining the data needed, and completing and reviewing the collection information. Send comments regarding this burden estimate or any other aspect of this collection of information, including suggestions for reducing the burden, to Department of Defense, Washington Headquarters Services, Directorate for Information Operations and Reports (0704-0188), 1215 Jefferson Davis Highway, Suite 1204, Arlington, VA 22202-4302. Respondents should be aware that notwithstanding any other provision of law, no person shall be subject to any penalty for failing to comply with a collection of information if it does not display a currently valid OMB control number.

**PLEASE DO NOT RETURN YOUR FORM TO THE ABOVE ADDRESS.**

<b>1. REPORT DATE (DD-MM-YYYY)</b> April 2020		<b>2. REPORT TYPE</b> Technical Note		<b>3. DATES COVERED (From - To)</b> January–March 2020	
<b>4. TITLE AND SUBTITLE</b> Low-Noise Amplifiers (LNAs) and Power Amplifiers (PAs) for Next-Generation S- and X-Band Radars' Testing				<b>5a. CONTRACT NUMBER</b>	
				<b>5b. GRANT NUMBER</b>	
				<b>5c. PROGRAM ELEMENT NUMBER</b>	
<b>6. AUTHOR(S)</b> John E Penn				<b>5d. PROJECT NUMBER</b>	
				<b>5e. TASK NUMBER</b>	
				<b>5f. WORK UNIT NUMBER</b>	
<b>7. PERFORMING ORGANIZATION NAME(S) AND ADDRESS(ES)</b> CCDC Army Research Laboratory ATTN: FCDD-RLS-ER Aberdeen Proving Ground, MD 21005				<b>8. PERFORMING ORGANIZATION REPORT NUMBER</b>  ARL-TN-1014	
<b>9. SPONSORING/MONITORING AGENCY NAME(S) AND ADDRESS(ES)</b>				<b>10. SPONSOR/MONITOR'S ACRONYM(S)</b>	
				<b>11. SPONSOR/MONITOR'S REPORT NUMBER(S)</b>	
<b>12. DISTRIBUTION/AVAILABILITY STATEMENT</b> Approved for public release; distribution is unlimited.					
<b>13. SUPPLEMENTARY NOTES</b> ORCID ID(s): John E Penn, 0000-0001-7535-0388					
<b>14. ABSTRACT</b> The US Army Combat Capabilities Development Command (CCDC) Army Research Laboratory (ARL) has been evaluating and designing efficient broadband high-power amplifiers for future adaptive, multimode radar systems in addition to other circuits for use in communications, networking, and electronic warfare (EW). The CCDC Army Research Laboratory submitted designs of broadband amplifiers, power amplifiers, high-dynamic-range low-noise amplifiers, high-power switches, frequency multipliers, and other circuits for future radar, communications, EW, and sensor systems using Qorvo Inc.'s high-performance 0.15-μm gallium nitride (GaN) fabrication process. This technical note summarizes the testing of multiple designs using Qorvo's 0.15-μm high-power, efficient GaN on a 4-mil silicon carbide process that was submitted to an ARL Prototype Wafer Option fabrication.					
<b>15. SUBJECT TERMS</b> Monolithic Microwave Integrated Circuit, MMIC, power amplifier, low-noise amplifier, microwave, radar					
<b>16. SECURITY CLASSIFICATION OF:</b>			<b>17. LIMITATION OF ABSTRACT</b>  UU	<b>18. NUMBER OF PAGES</b>  59	<b>19a. NAME OF RESPONSIBLE PERSON</b> John E Penn
<b>a. REPORT</b> Unclassified	<b>b. ABSTRACT</b> Unclassified	<b>c. THIS PAGE</b> Unclassified			<b>19b. TELEPHONE NUMBER (Include area code)</b> (301) 394-0423

## **Contents**

---

<b>List of Figures</b>	<b>iv</b>
<b>Acknowledgments</b>	<b>vi</b>
<b>1. Introduction</b>	<b>1</b>
<b>2. S- and X-Band Low-Noise Amplifier</b>	<b>1</b>
<b>3. S- and X-Band Power Amplifier</b>	<b>5</b>
<b>4. S- and X-Band 10-W PA</b>	<b>12</b>
<b>5. Broadband Feedback Amplifiers</b>	<b>20</b>
<b>6. Broadband Nonuniform Distributed Amplifier</b>	<b>37</b>
<b>7. Other Broadband-Amplifier Test Circuits</b>	<b>40</b>
<b>8. Conclusions</b>	<b>48</b>
<b>9. References</b>	<b>49</b>
<b>List of Symbols, Abbreviations, and Acronyms</b>	<b>50</b>
<b>Distribution List</b>	<b>51</b>

## List of Figures

Fig. 1	S- and X-band LNA photo ( $1.3 \times 1.1$ mm).....	2
Fig. 2	S- and X-band LNA measured (solid) vs. simulation (dash) 6- $\times$ 25- $\mu$ m LNA (5 V) .....	3
Fig. 3	S- and X-band LNA measured (solid) vs. simulation (dash) 6- $\times$ 25- $\mu$ m LNA (10 V) .....	4
Fig. 4	Photo of S- and X-band PA ( $1.8 \times 1.0$ mm) .....	5
Fig. 5	S- and X-band PA measured (solid) vs. simulation (dash) 8- $\times$ 150- $\mu$ m PA (20 and 28 V) .....	6
Fig. 6	Measured (solid) vs. simulation (dash) 3.5- to 6-GHz PA (20 V).....	8
Fig. 7	Measured (solid) vs. simulation (dash) 3.5- to 6-GHz PA (28 V).....	9
Fig. 8	Measured PAE (magenta), gain (blue) vs. power output, 8- $\times$ 150- $\mu$ m PA (20 V) .....	10
Fig. 9	Measured PAE (magenta), gain (blue) vs. power output, 8- $\times$ 150- $\mu$ m PA (28 V) .....	11
Fig. 10	Photo of S- and X-band two-way 8- $\times$ 150- $\mu$ m 10-W PA ( $1.8 \times 1.3$ mm) .....	12
Fig. 11	S- and X-band PA measured (solid) vs. simulation (dash) two-way 8- $\times$ 150- $\mu$ m PA (20 and 28 V).....	13
Fig. 12	S- and X-band PA measured (solid) vs. simulation (dash) 10-W PA (fixture 28 V) .....	14
Fig. 13	Measured (solid) vs. simulation (dash) 4-GHz, 10-W PA (die 20 V)	16
Fig. 14	Measured (solid) vs. simulation (dash) 4-GHz, 10-W PA (die 28 V)	17
Fig. 15	Measured PAE (magenta) and gain (blue) vs. power output, 3.5- to 8-GHz, 10-W PA (fixture 20 V).....	18
Fig. 16	Measured PAE (magenta) and gain (blue) vs. power output, 3.5- to 8-GHz, 10-W PA (fixture 28 V).....	19
Fig. 17	Photo of feedback amplifiers plus S- and X-band LNA ( $2 \times 2$ mm)..	21
Fig. 18	Measured (solid) vs. simulation (dash) of 6- $\times$ 50- $\mu$ m resistive- feedback amplifier .....	22
Fig. 19	Measured (solid) vs. simulation (dash) of 4- $\times$ 50- $\mu$ m source-feedback amplifier (10 V) .....	23
Fig. 20	Measured (solid) vs. simulation (dash) of 4- $\times$ 65- $\mu$ m source-feedback amplifier (10 V) .....	24
Fig. 21	Measured (solid) vs. simulation (dash) at 6 GHz, 6- $\times$ 50- $\mu$ m amplifier (10 and 20 V) .....	26

Fig. 22	Measured (solid) vs. simulation (dash) at 8 GHz, 6- × 50-μm amplifier (10 and 20 V) .....	27
Fig. 23	Measured (solid) vs. simulation (dash) at 10 GHz, 6- × 50-μm amplifier (10 and 20 V).....	28
Fig. 24	Measured (solid) vs. simulation (dash) at 6 GHz, 4- × 50-μm amplifier (10 and 20 V) .....	30
Fig. 25	Measured (solid) vs. simulation (dash) at 8 GHz, 4- × 50-μm amplifier (10 and 20 V) .....	31
Fig. 26	Measured (solid) vs. simulation (dash) at 10 GHz, 4- × 50-μm amplifier (10 and 20 V).....	32
Fig. 27	Measured (solid) vs. simulation (dash) at 6 GHz, 4- × 65-μm amplifier (10 and 20 V) .....	34
Fig. 28	Measured (solid) vs. simulation (dash) at 8 GHz, 4- × 65-μm amplifier (10 and 20 V) .....	35
Fig. 29	Measured (solid) vs. simulation (dash) at 10 GHz, 4- × 65-μm amplifier (10 and 20 V).....	36
Fig. 30	Photo of nonuniform distributed amplifier (NUDA), 1.5 × 1.0 mm...	37
Fig. 31	Measured (solid) vs. simulation (dash) of NUDA (10 V) .....	38
Fig. 32	Measured (solid) vs. simulation (dash) of NUDA (20 V) .....	39
Fig. 33	Photo of cascode DA (1.3 × 0.6 mm) .....	40
Fig. 34	Measured (solid) vs. simulation (dash) of cascode DA (20 V).....	41
Fig. 35	Photo of 4- × 110-μm feedback broadband amplifier (0.5 × 0.6 mm)	42
Fig. 36	Measured (solid) vs. simulation (dash) of 4- × 110-μm feedback amplifier (10, 20 V) .....	43
Fig. 37	Measured (solid) vs. simulation (dash) at 6 GHz, 4- × 110-μm amplifier (10 and 20 V).....	45
Fig. 38	Measured (solid) vs. simulation (dash) at 8 GHz, 4- × 110-μm amplifier (10 and 20 V).....	46
Fig. 39	Measured (solid) vs. simulation (dash) at 10 GHz, 4- × 110-μm amplifier (10 and 20 V).....	47

## **Acknowledgments**

---

---

Khamsouk Kingkeo assembled and packaged all of the die for testing, took the die photos, and helped with all the testing and data transfers. Sami Hawasli wrote software that made performance testing much quicker, more efficient, and more accurate. Dr Ali Darwish has many great ideas for designs and is the Team Lead for our III/V Monolithic Microwave Integrated Circuit design team.

## **1. Introduction**

---

---

The US Army Combat Capabilities Development Command (CCDC) Army Research Laboratory (ARL) has been evaluating and designing efficient, broadband high-power amplifiers and robust low-noise amplifiers (LNAs) for future multimode radar systems that could be used in other applications such as communications, networking, and electronic warfare (EW). CCDC Army Research Laboratory submitted designs of broadband amplifiers, power amplifiers, and high-dynamic-range LNAs for future radar, communications, EW, and sensor systems using Qorvo Inc's high-performance, 0.15- $\mu\text{m}$  gallium nitride (GaN) fabrication process. The testing and analysis of circuits most applicable to radar applications, as well as lessons learned for improvements to future design efforts, are documented in this technical note. (See ARL-TR-8871 for documentation of these designs.<sup>1</sup>)

## **2. S- and X-Band Low-Noise Amplifier**

---

---

An LNA was designed for gain, noise figure, bandwidth, and stability over about 3–10 GHz using a 6-  $\times$  25- $\mu\text{m}$  high electron mobility transistor (HEMT) model that contained noise data for DC biases of 5 and 10 V. These designs should be able to operate over a large range of DC, though the best noise figure is typically at a moderately low drain current ( $I_{\text{DS}}$ ), typically 100–150m A/mm. Figure 1 shows a picture of the LNA monolithic microwave integrated circuit (MMIC).

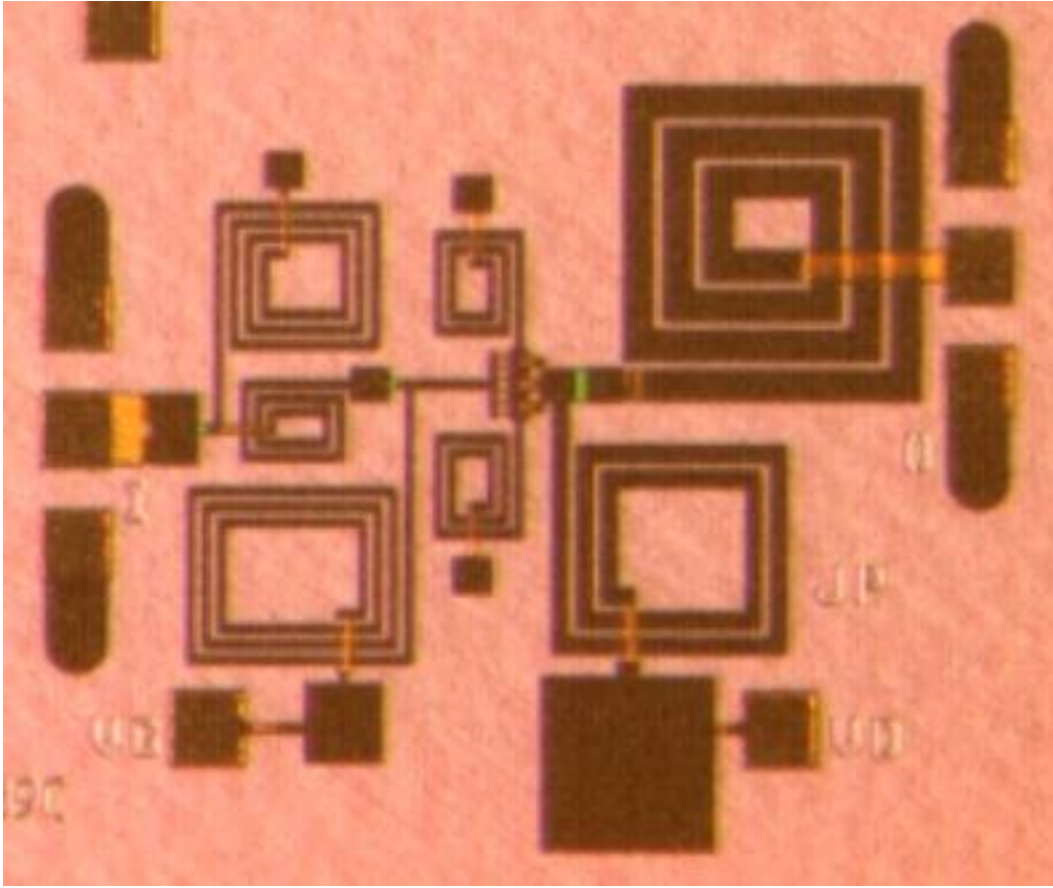


**Fig. 1 S- and X-band LNA photo (1.3 × 1.1 mm)**

Figure 2 shows a plot of measurements (solid line) versus simulations (dashed line) of the small signal s-parameters of the first-stage  $6\text{-} \times 25\text{-}\mu\text{m}$  LNA at the nominal 5-V DC bias. The shapes are very similar, except the gain starts a little higher than the desired 3 GHz. Figure 3 shows a plot of measurements (solid) versus simulations (dash) of the small signal s-parameters of the first-stage  $6\text{-} \times 25\text{-}\mu\text{m}$  LNA at the nominal 10-V DC bias. The gain is significantly lower than expected at 10 V, but the return loss matches well with the linear HEMT model. An electromagnetic (EM) resimulation of the full one-stage LNA layout was created to eliminate the possibility of unsimulated parasitic interaction among the input match, source inductance, and output match of this very compact layout. Yet, the full EM layout's result was similar to the original simulation, where those three EM layouts were isolated subcircuits. Noise-figure measurements were not completed and will be delayed. Original simulations predicted a noise figure of 1.3–1.6 dB from 3 to 13 GHz.

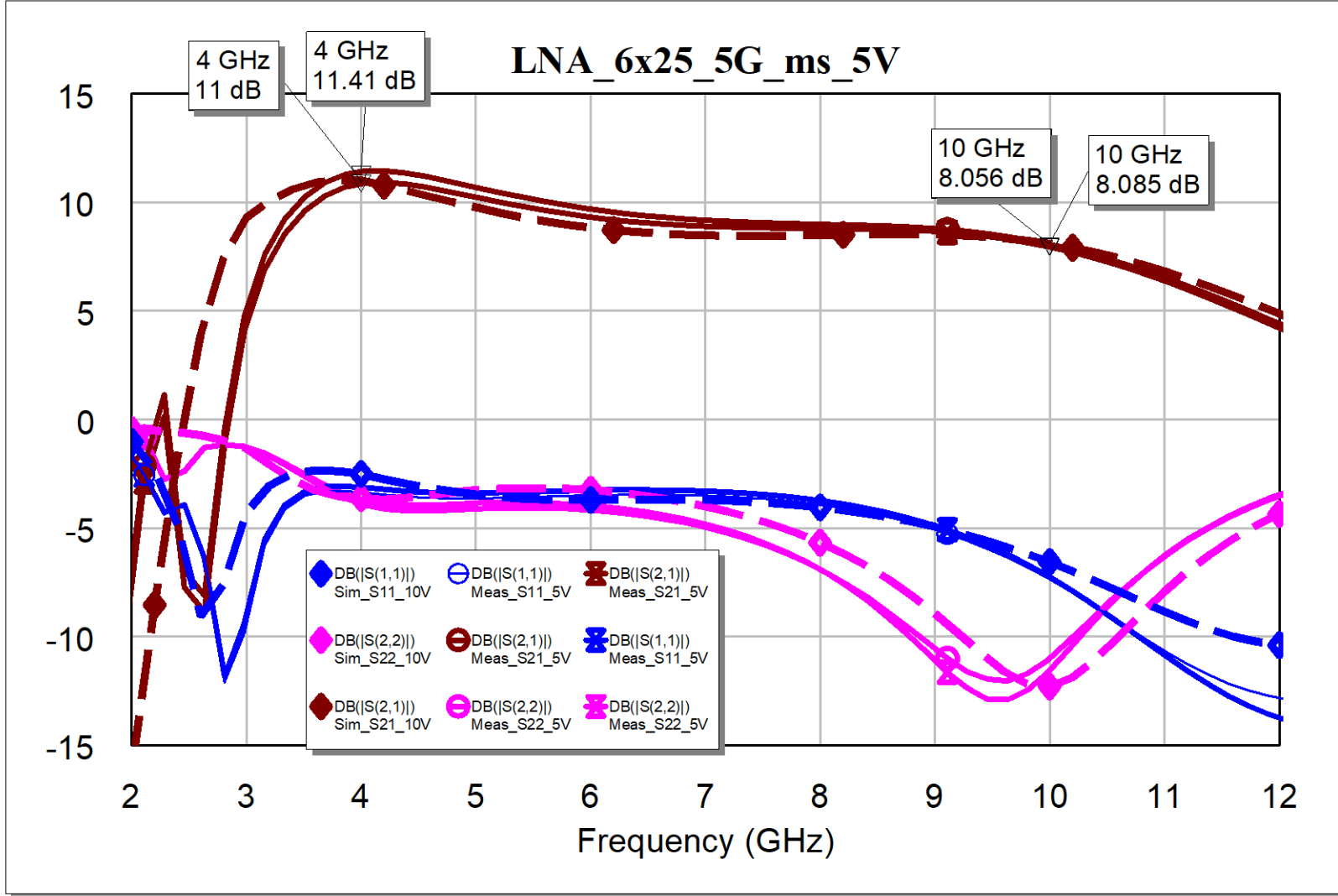
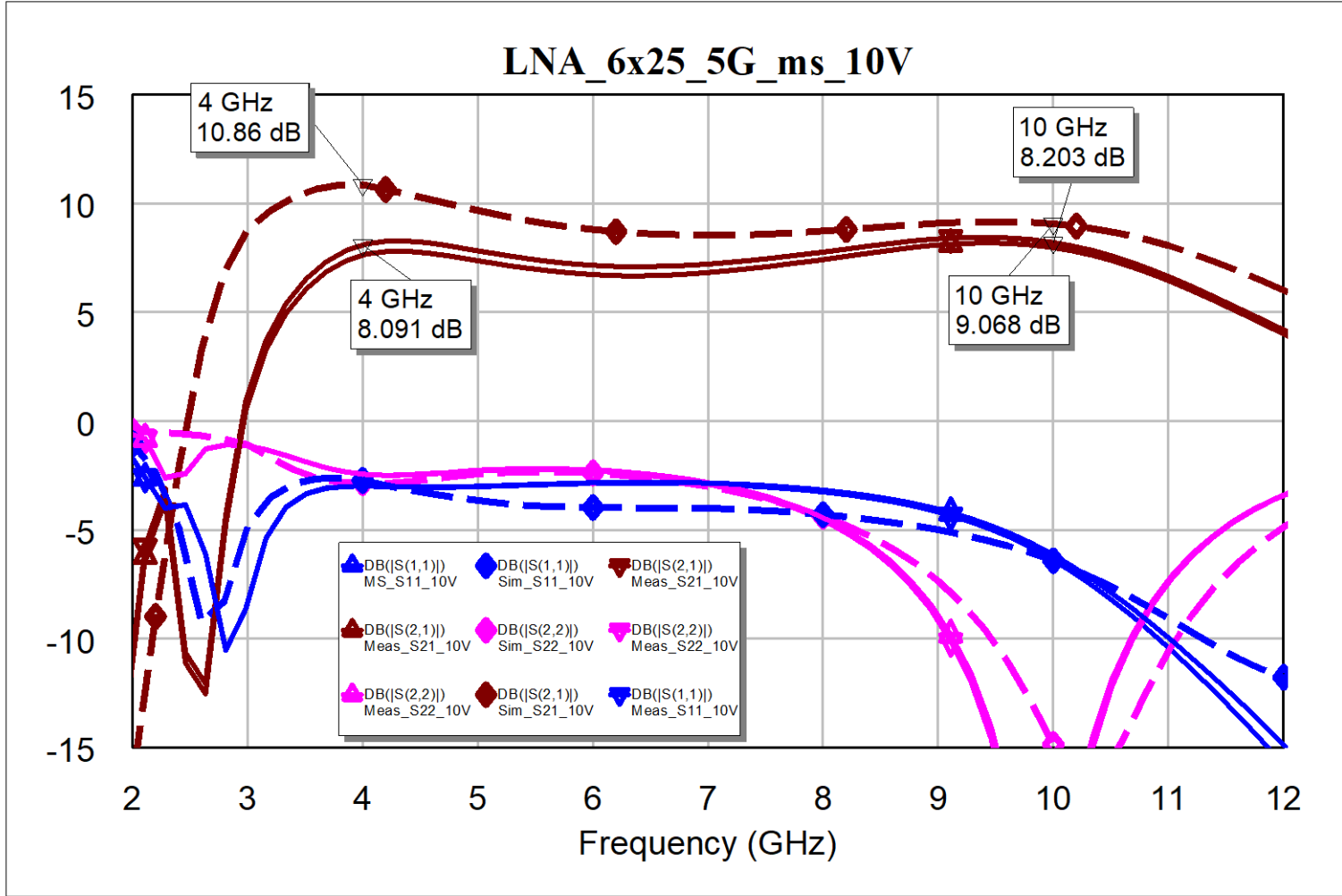


Fig. 2 S- and X-band LNA measured (solid) vs. simulation (dash) 6- × 25- $\mu$ m LNA (5 V)



**Fig. 3** S- and X-band LNA measured (solid) vs. simulation (dash)  $6 \times 25\text{-}\mu\text{m}$  LNA (10 V)

### 3. S- and X-Band Power Amplifier

---

An S- and X-band power amplifier (PA) with an  $8\text{-}\times\text{150-}\mu\text{m}$  HEMT to target a power goal of 5 W was designed, fabricated, and tested, yielding good gain, efficiency, bandwidth, and stability over 3 to 10 GHz for DC biases of 28 V, or 20 V for less power. These designs should operate over a large range of DC, though the best power and efficiency should be at 28 V, at a nominal  $I_{DS}$  of 100–150 mA/mm. Figure 4 shows a picture of the PA MMIC.

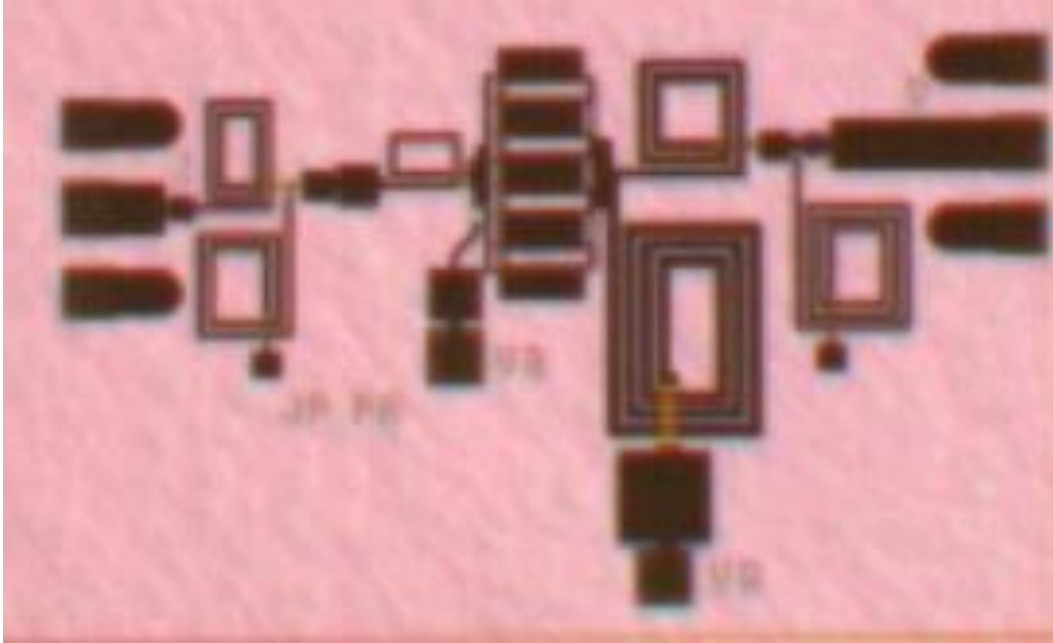


**Fig. 4** Photo of S- and X-band PA (1.8  $\times$  1.0 mm)

Figure 5 shows a plot of measurements (solid) versus simulations (dash) of the small signal s-parameters of the one-stage  $8\text{-}\times\text{150-}\mu\text{m}$  PA at 20- and 28-V DC bias. The simulation at 25 V matches well with the measured amplifier.

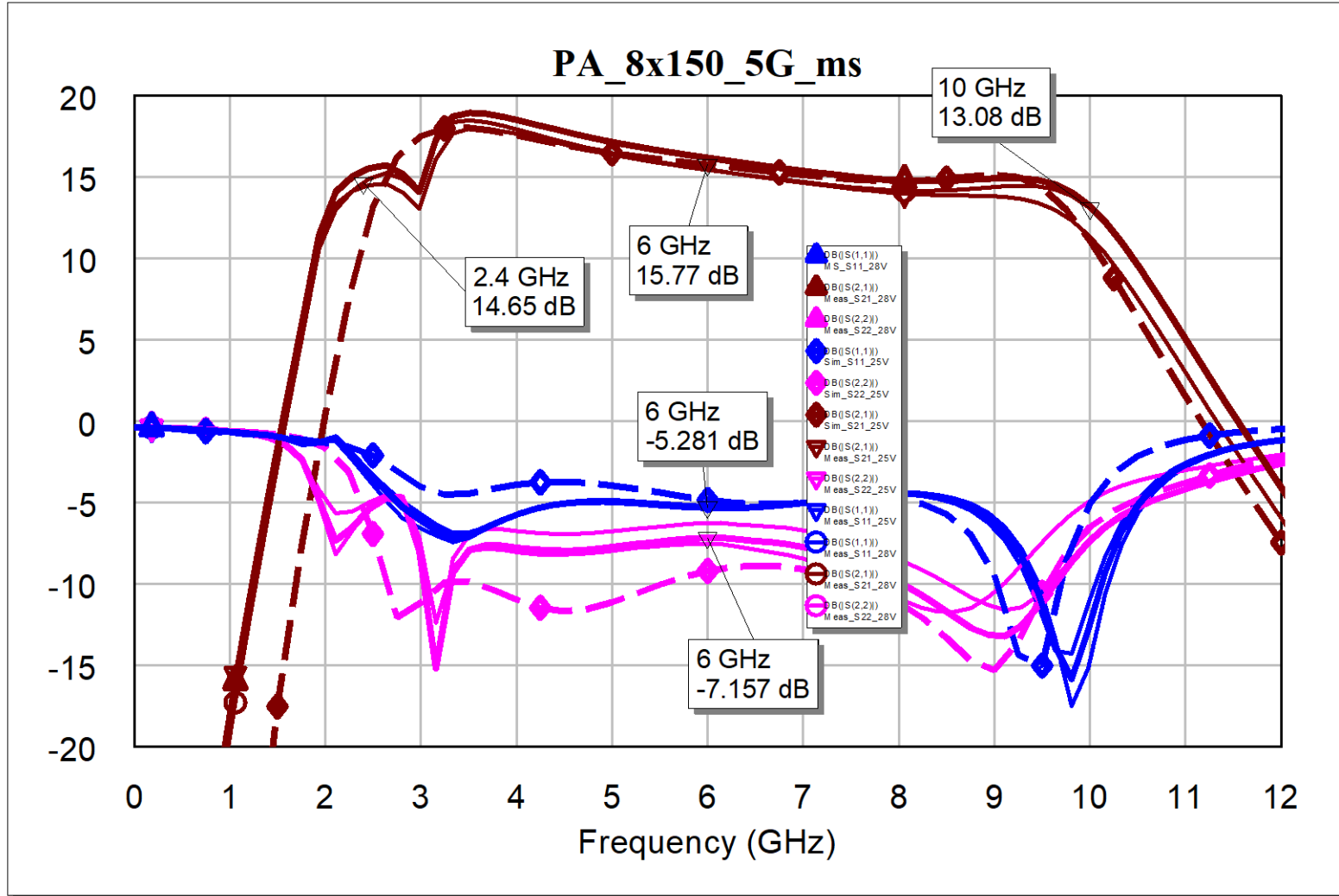


Fig. 5 S- and X-band PA measured (solid) vs. simulation (dash) 8- × 150-μm PA (20 and 28 V)

Power measurements of the one-stage PAs were performed at 20 and 28 V. Figure 6 shows output power (blue), power-added efficiency (PAE; magenta), and gain (brown) measured in (solid) versus simulation (dash) plots of the  $8 \times 150\text{-}\mu\text{m}$  PA at the 20-V DC bias and at frequencies from 3.5 to 6 GHz (see figure's legend). Measurements were taken up to 8 GHz but matched better up to 6 GHz, as the performance was below expectations from 7 to 8 GHz. The simulations at 3, 6, and 9 GHz predicted 45%–50% PAE with output powers greater than 35 dBm (3 W). In the future, these PAs should be tested above 8 GHz, up to 10 GHz, for power performance and also remeasured from 6 to 8 GHz to eliminate measurement error in the preliminary measurements. Also, load-pull measurements should be performed to verify the accuracy of the nonlinear models used for this design and for use in improving performance in a future redesign or for a customized tweak of the output match to achieve optimal performance within a package. PAE is very good with 40%–49% peak, while output powers reach 3 W (35 dBm). Similarly, Fig. 7 shows output power (blue), PAE (magenta), and gain (brown) measured in (solid) versus simulation (dash) plots of the  $8 \times 150\text{-}\mu\text{m}$  PA at the desired 28-V DC bias and at frequencies from 3.5 to 6 GHz (see legend). PAE is very good with 37%–45% peak, while output powers reach 5 W (37 dBm). While the current measurements show less than expected performance at 7–8 GHz, the output powers are good, achieving nearly 3 W (35 dBm) at 20 V and 5 W at 28 V from 3.5 to 8 GHz. Replotting PAE (magenta) and large signal gain (blue) versus measured output power is shown in Fig. 8 for the PA at 20V. Software written by Sami Hawasli was very helpful in stepping quickly through power levels and over 0.5-GHz frequency steps. Khamsouk Kingkeo helped with all of the measurements and also assembled the amplifier dice on a small piece of metal for probe testing, adding wire bonds to DC decoupling capacitors. A similar plot of PAE (magenta) and large signal gain (blue) versus measured output power is shown in Fig. 9 for the PA at 28V from 3.5 to 8 GHz in 0.5-GHz steps. The goal of 5 W (37 dBm) is achieved, or nearly achieved, as all of these measured frequencies. Ideally, the measurements should all be driven up to the peak PAE; here, in some cases, PAE is still rising and has not achieved a peak. Efficiencies are good over such a broad band, ranging from 30% to 45% PAE.

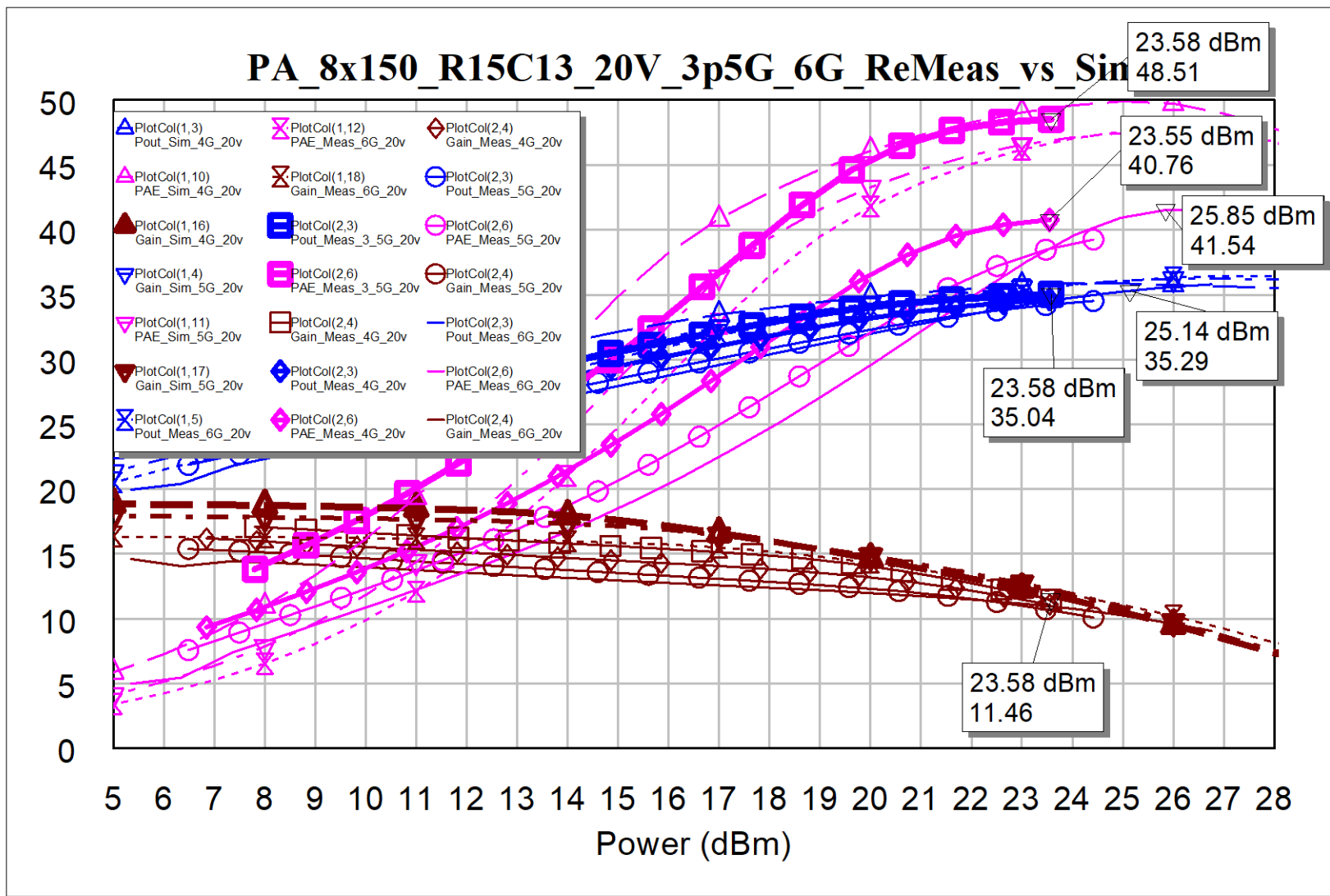
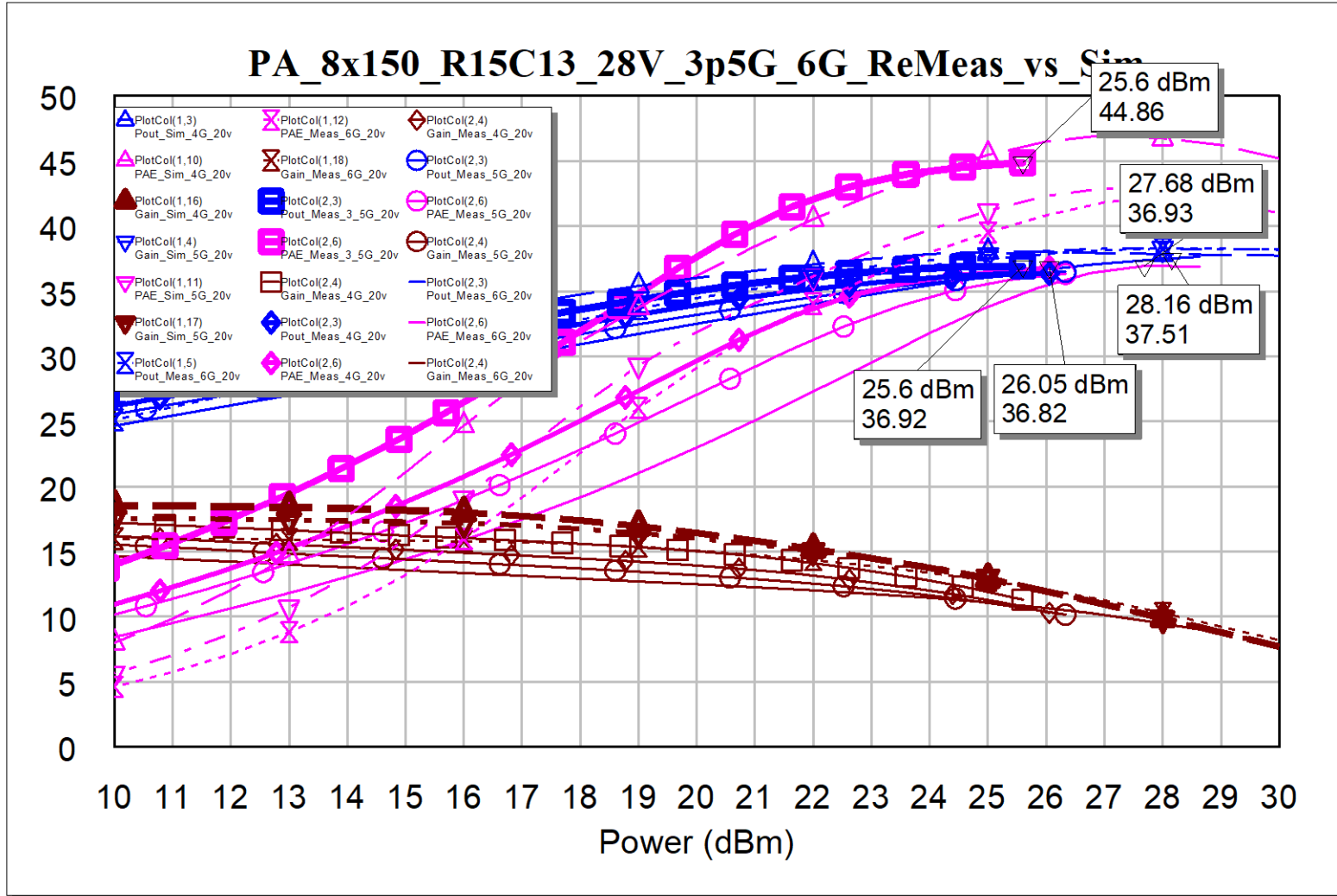
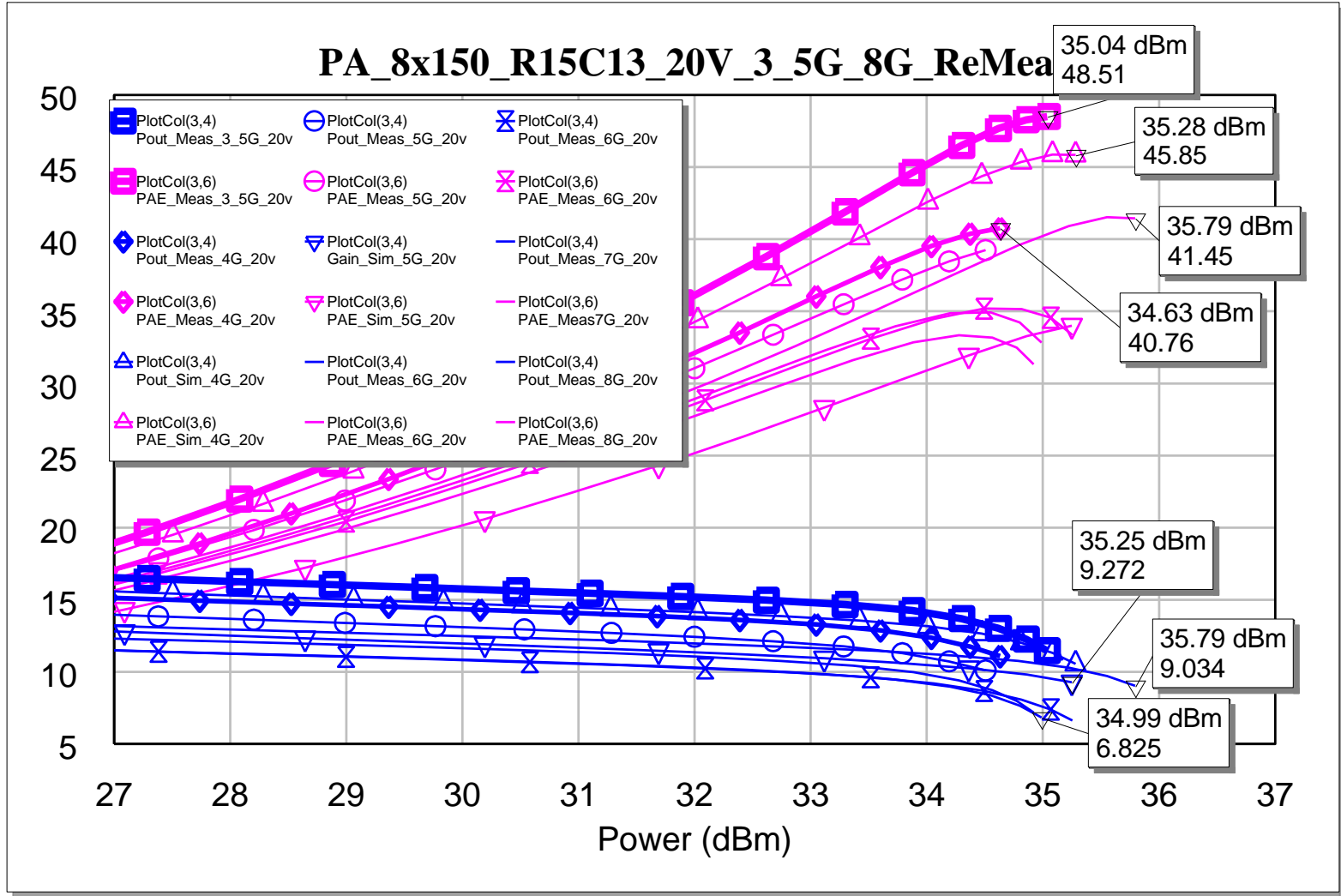


Fig. 6 Measured (solid) vs. simulation (dash) 3.5- to 6-GHz PA (20 V)



**Fig. 7 Measured (solid) vs. simulation (dash) 3.5- to 6-GHz PA (28 V)**



**Fig. 8 Measured PAE (magenta), gain (blue) vs. power output, 8- × 150- $\mu$ m PA (20 V)**

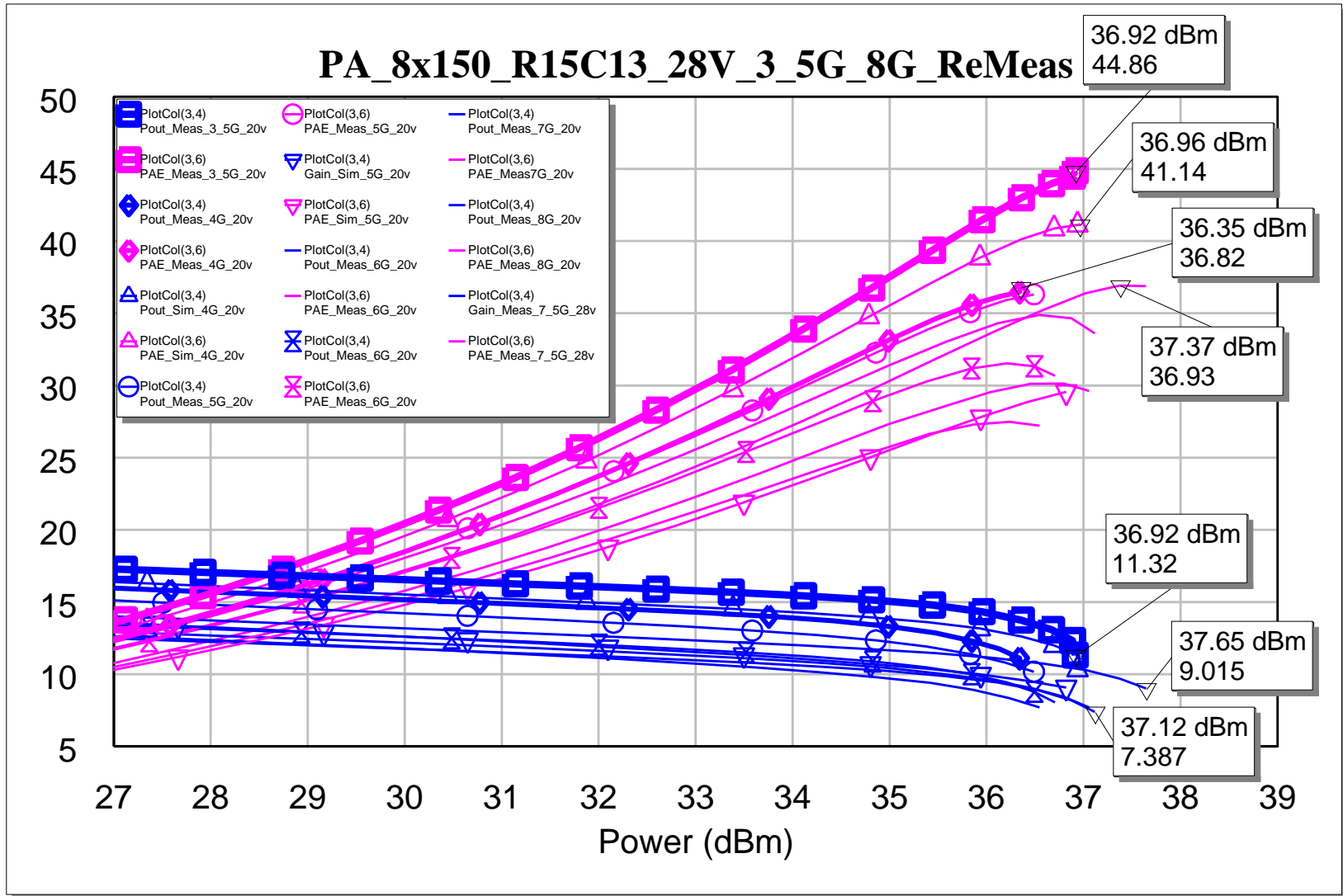
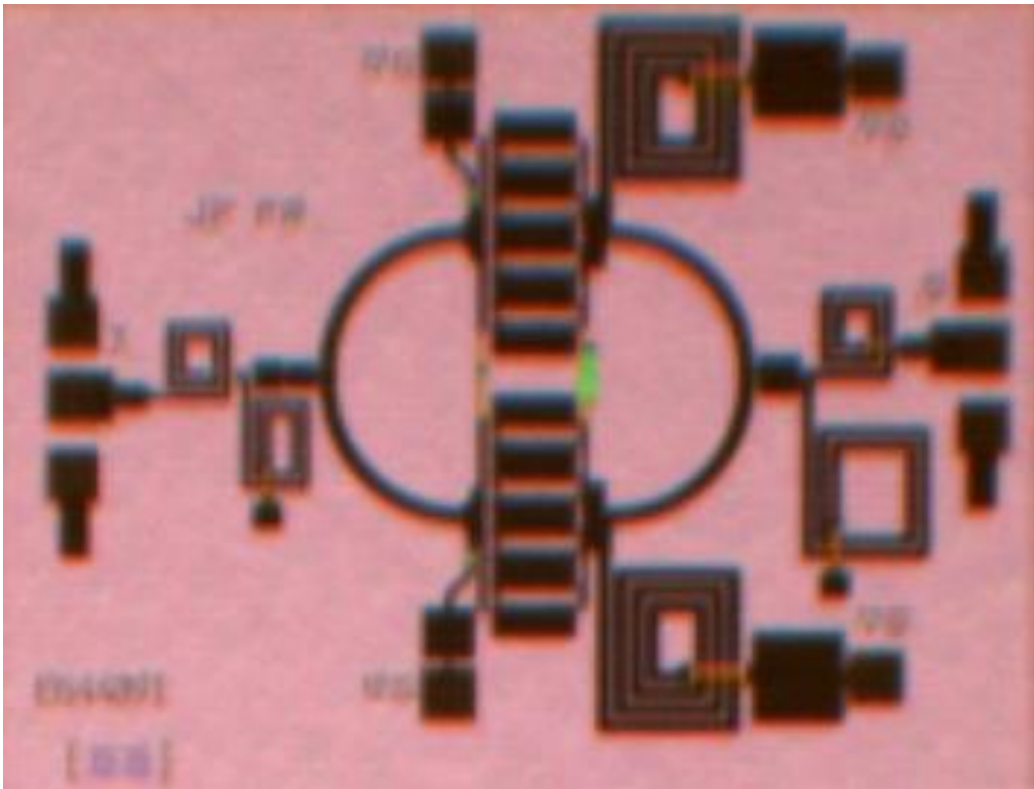


Fig. 9 Measured PAE (magenta), gain (blue) vs. power output, 8- x 150-um PA (28 V)

#### 4. S- and X-Band 10-W PA

---

The single  $8\text{-}\times\text{150-}\mu\text{m}$  HEMT 5- to 6-W S- and X-band PA design was used as the basis for parallel combining two  $8\text{-}\times\text{150-}\mu\text{m}$  HEMTs to achieve a 10-W output power goal. A picture of the two-way combined  $8\text{-}\times\text{150-}\mu\text{m}$  PA MMIC is shown in Fig. 10. Figure 11 shows a plot of measurements (solid) versus simulations (dash) of the small signal s-parameters of the 10-W PA at 20- and 28-V DC bias, with the best match to simulations at 28 V even though the simulation is at 20 V. The high-power MMIC was packaged on a fixture with comparable performance and also because the die measurements were exceeding the 10-W power limitation of the coplanar probes. When tested in a connectorized package, as shown in Fig. 12, there was good agreement in the plot of measurements (solid) versus simulations (dash) of the small signal s-parameters of the 10-W PA at 28-V DC bias; again, the simulation is at 20 V. At these frequencies, the measurements are nearly identical to the probed die of the 10-W PA.



**Fig. 10** Photo of S- and X-band two-way  $8\text{-}\times\text{150-}\mu\text{m}$  10-W PA ( $1.8\text{ }\times\text{ }1.3\text{ mm}$ )

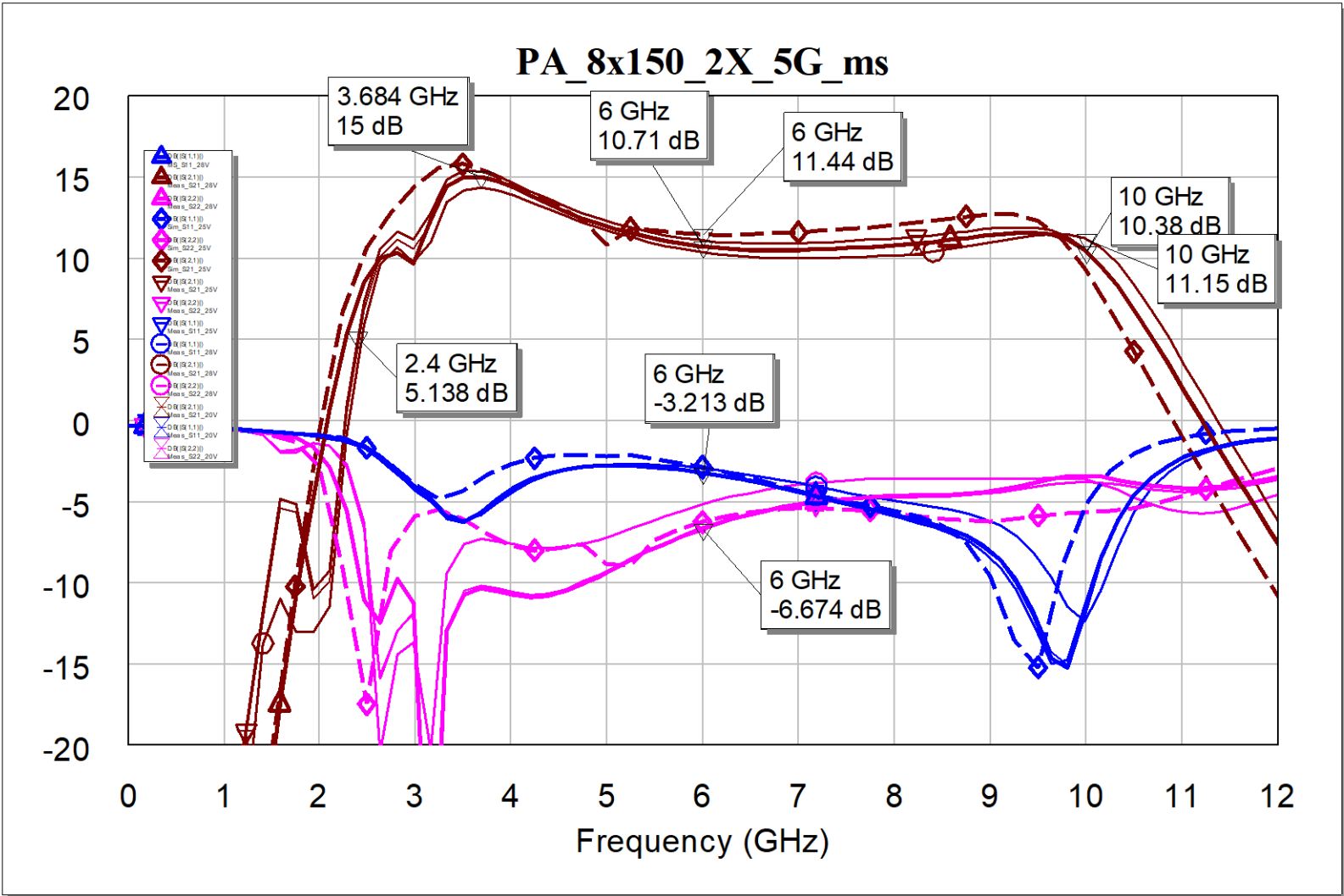


**Fig. 11** S- and X-band PA measured (solid) vs. simulation (dash) two-way 8- $\times$ 150- $\mu$ m PA (20 and 28 V)

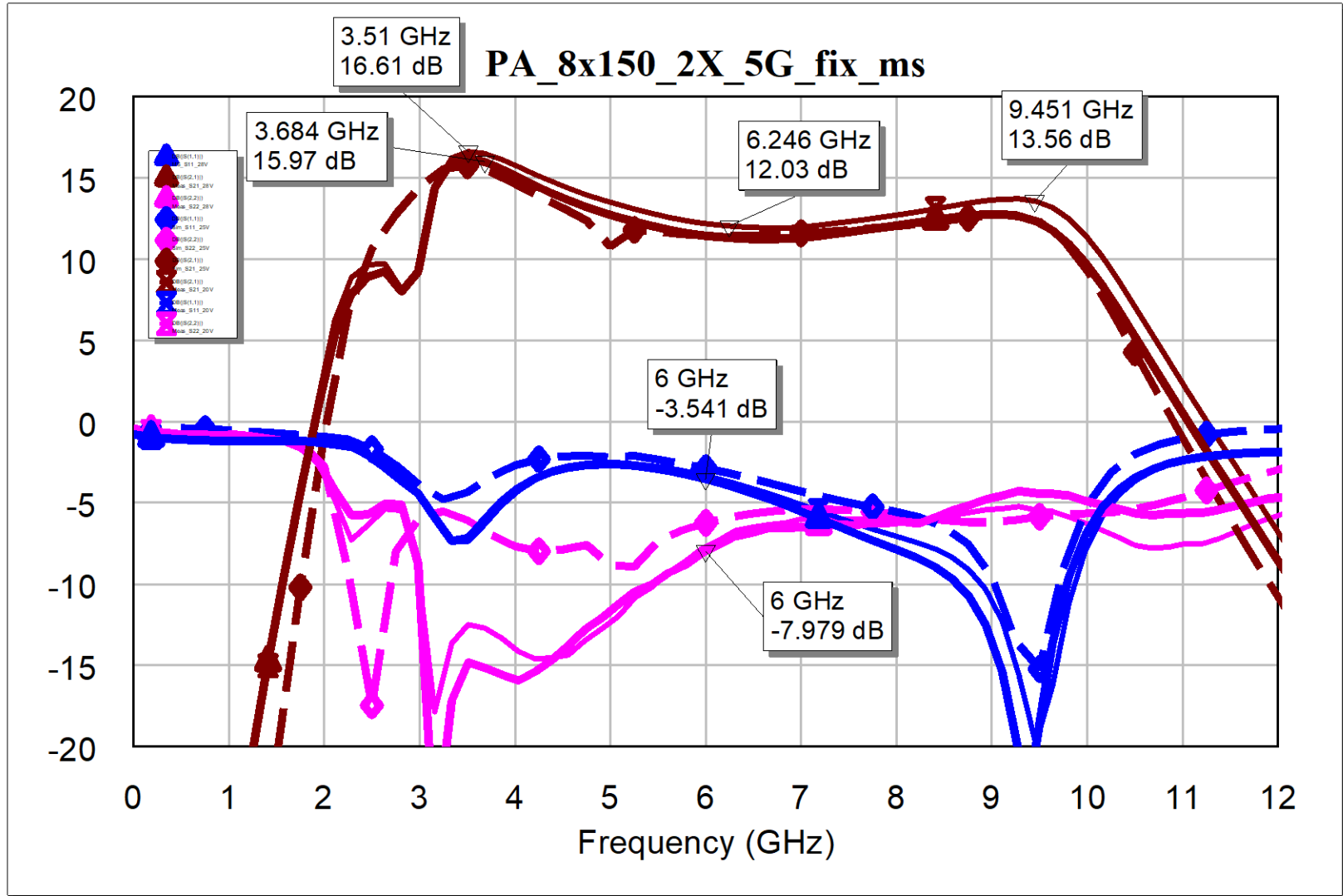


Fig. 12 S- and X-band PA measured (solid) vs. simulation (dash) 10-W PA (fixture 28 V)

Power measurements of the one-stage PAs were performed at 20 and 28 V. Figure 13 shows output power (blue), PAE (magenta), and gain (brown) measured in (solid) versus simulation (dash) plots of the two-way  $8 \times 150\text{-}\mu\text{m}$  PA at the 20-V DC bias and at 4 GHz measured as a probed die (see legend). The PA achieved excellent 53% PAE with an output power greater than 37.8 dBm (6 W). As with the single  $8 \times 150\text{-}\mu\text{m}$  HEMT PA, this 10-W PA should be tested above 8 GHz, up to 10 GHz, for power performance using a fixture as the output power exceeds the probe limits. Also, load-pull measurements should be performed as well. Similarly, Fig. 14 shows output power (blue), PAE (magenta), and gain (brown) in measured (solid) versus simulation (dash) plots of the two-way  $8 \times 150\text{-}\mu\text{m}$  PA at the desired 28-V DC bias and at 4 GHz measured as a probed die (see legend). PAE is excellent with a 51% peak, while achieving an output power of 10 W (40 dBm). Once packaged, the 10-W PA was measured at 20 V and 28 V from 3.5 to 8 GHz in 0.5-GHz steps. Plotting PAE (magenta) and large signal gain (blue) versus measured output power is shown in Fig. 15 for the PA at 20 V. Software written by Sami Hawasli was very helpful in stepping quickly through power levels and frequency steps. Once again, Khamsouk Kingkeo helped with all of the measurements and in assembling the amplifiers on a connectorized fixture for testing. A similar plot of PAE (magenta) and large signal gain (blue) versus measured output power is shown in Fig. 16 for the PA at 28 V from 3.5 to 8 GHz in 0.5-GHz steps. The goal of 10 W (37 dBm) is achieved, with up to 51% PAE at the lower end of the band. Efficiencies are not as good as expected at the high end of the band. Additional measurements need to be taken of these designs to evaluate the differences for improving performance in a future redesign or with a tweaked, customized matching circuit within a package.

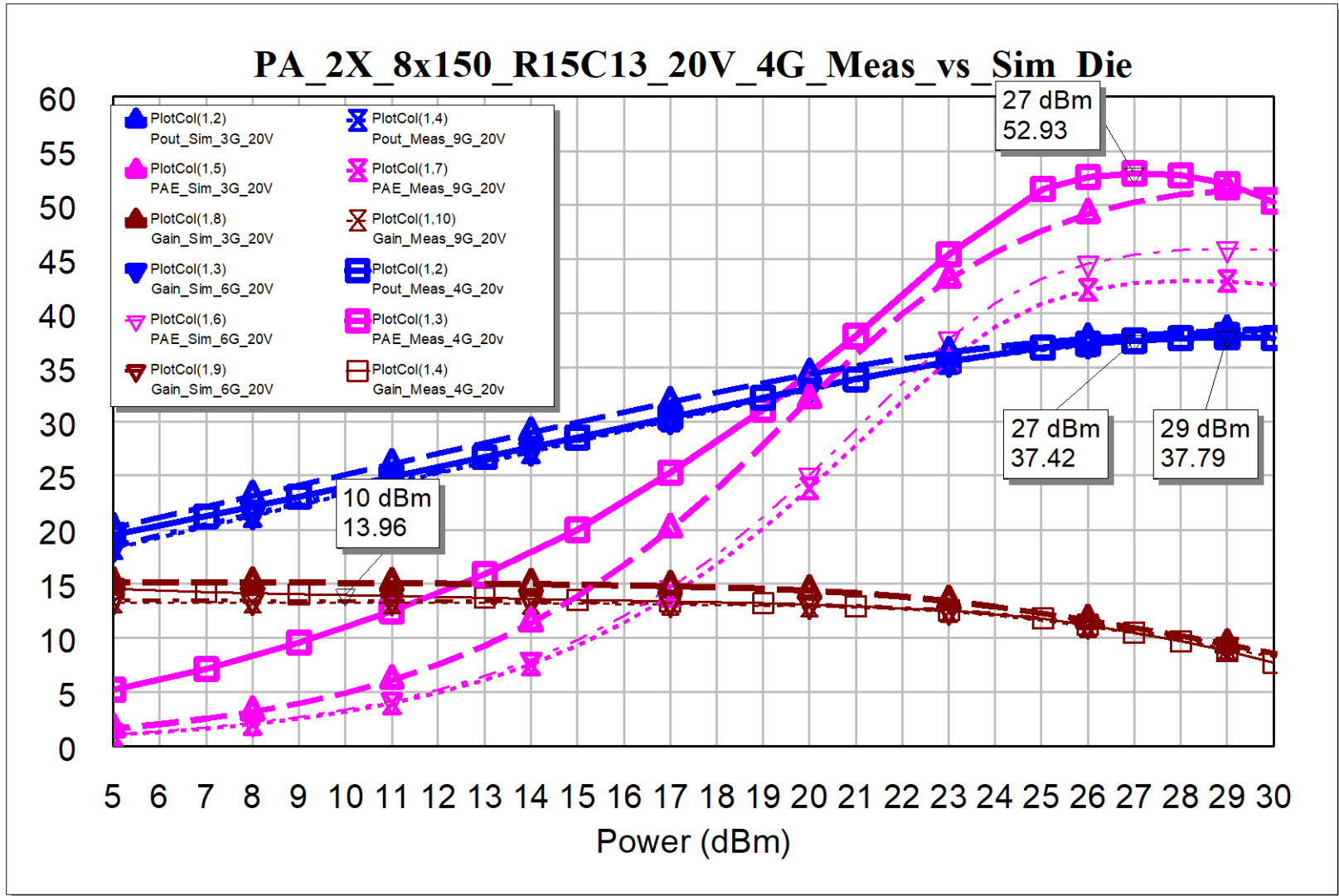


Fig. 13 Measured (solid) vs. simulation (dash) 4-GHz, 10-W PA (die 20 V)



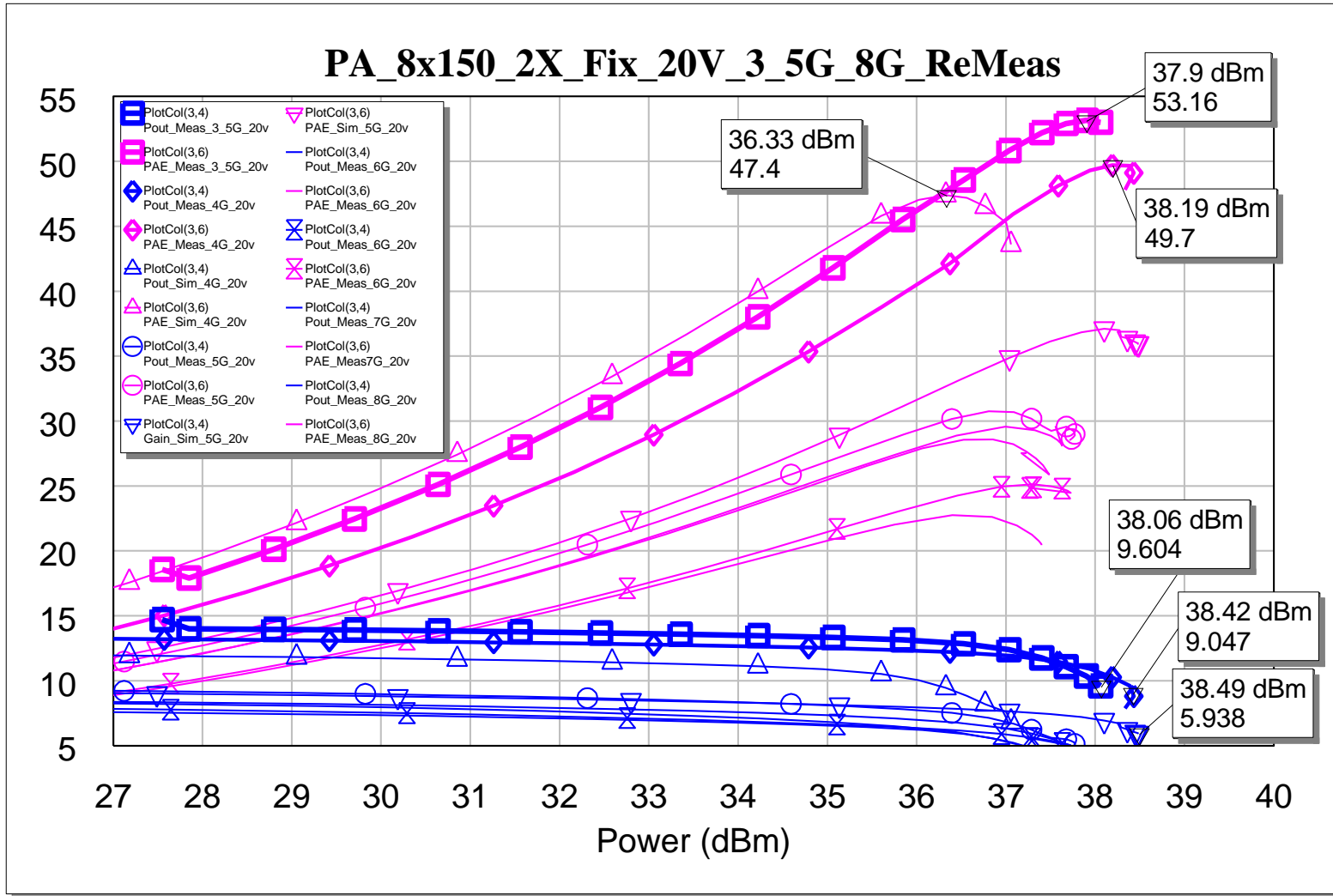


Fig. 15 Measured PAE (magenta) and gain (blue) vs. power output, 3.5- to 8-GHz, 10-W PA (fixture 20 V)

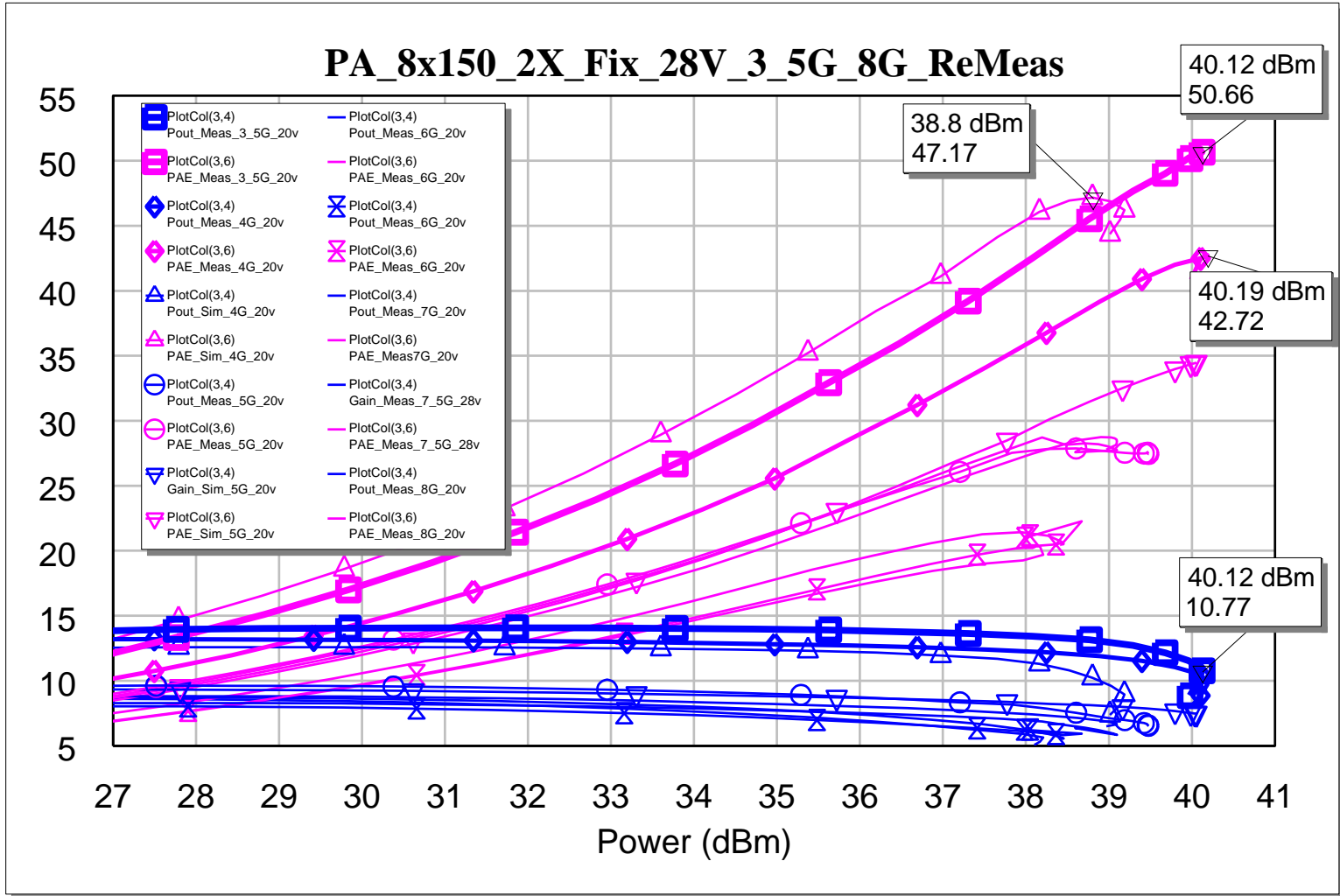


Fig. 16 Measured PAE (magenta) and gain (blue) vs. power output, 3.5- to 8-GHz, 10-W PA (fixture 28 V)

## 5. Broadband Feedback Amplifiers

---

A simple approach to a broadband amplifier uses feedback, typically resistive feedback from drain to gate. Several broadband-feedback amplifiers were designed in a prior Raytheon GaN process, demonstrating excellent noise figure as well as broadband gain. Using the two available noise-figure HEMT models for the Qorvo 0.15- $\mu\text{m}$  GaN process, variations of a broadband-feedback amplifier were designed. Figure 17 shows a picture of a 2-  $\times$  2-mm die that contains the three feedback amplifiers along the top and left sides, along with other test HEMTs and the previously mentioned S- and X-band LNA. The first amplifier uses a 6-  $\times$  50- $\mu\text{m}$  HEMT with resistive feedback, and the other two designs use source inductance to create broadband LNAs. Figure 18 shows measured (solid) versus simulations (dash) of the 6-  $\times$  50- $\mu\text{m}$  MMIC layout with broadband-gain performance, matching well with simulations at 5- and 10-V DC biases. Gain is still nearly 10 dB at 10 GHz, even higher at lower frequencies with 14-dB gain at 1 GHz. Next, measured (solid) versus simulations (dash) of the 4-  $\times$  50- $\mu\text{m}$  feedback amplifier using source feedback show good agreement (Fig. 19). This design also has 10-dB gain at 10 GHz, with up to 16-dB gain at 1 GHz, then falls off with frequency. Return loss of the source feedback design starts out poor at low frequency and gets better at increasing frequency, which is opposite of the prior resistive-feedback amplifier.

These designs would work over a range of operating voltages but were intended as broadband-gain amplifiers with low-noise performance at 5- to 10-V DC biases. They could make a broadband second stage combined with the prior low-noise S- and X-band LNA for a two-stage LNA or as a driver stage for a two-stage PA. Figure 20 shows measured (solid) versus simulations (dash) of the 4-  $\times$  65- $\mu\text{m}$  broadband amplifier, which also has 10-dB gain at 10 GHz and an even higher 18-dB gain at 1 GHz. While these amplifiers were not designed for power, or even simulated previously for power performance, they were measured at 6 to 12 GHz at 10- and 20-V DC biases for efficiency and output power.

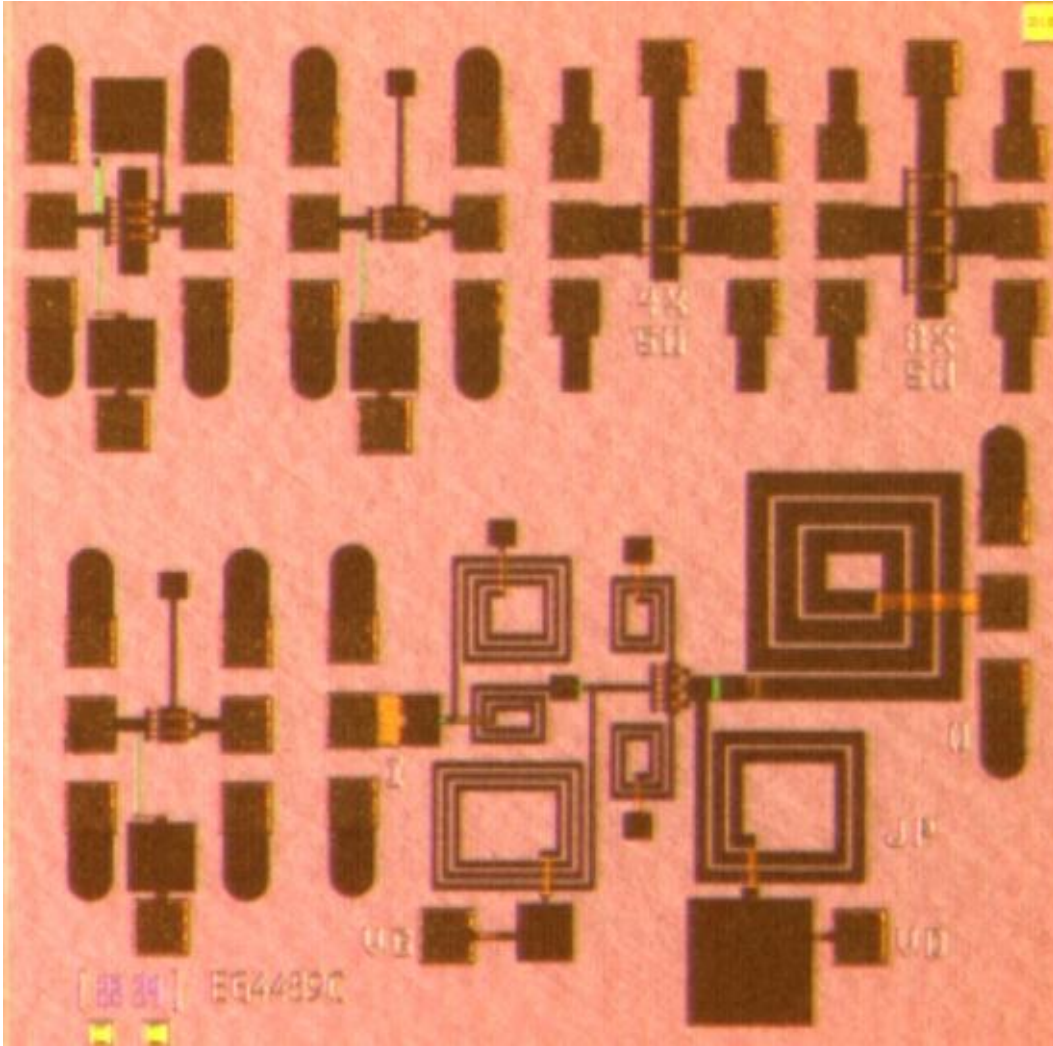


Fig. 17 Photo of feedback amplifiers plus S- and X-band LNA (2 × 2 mm)

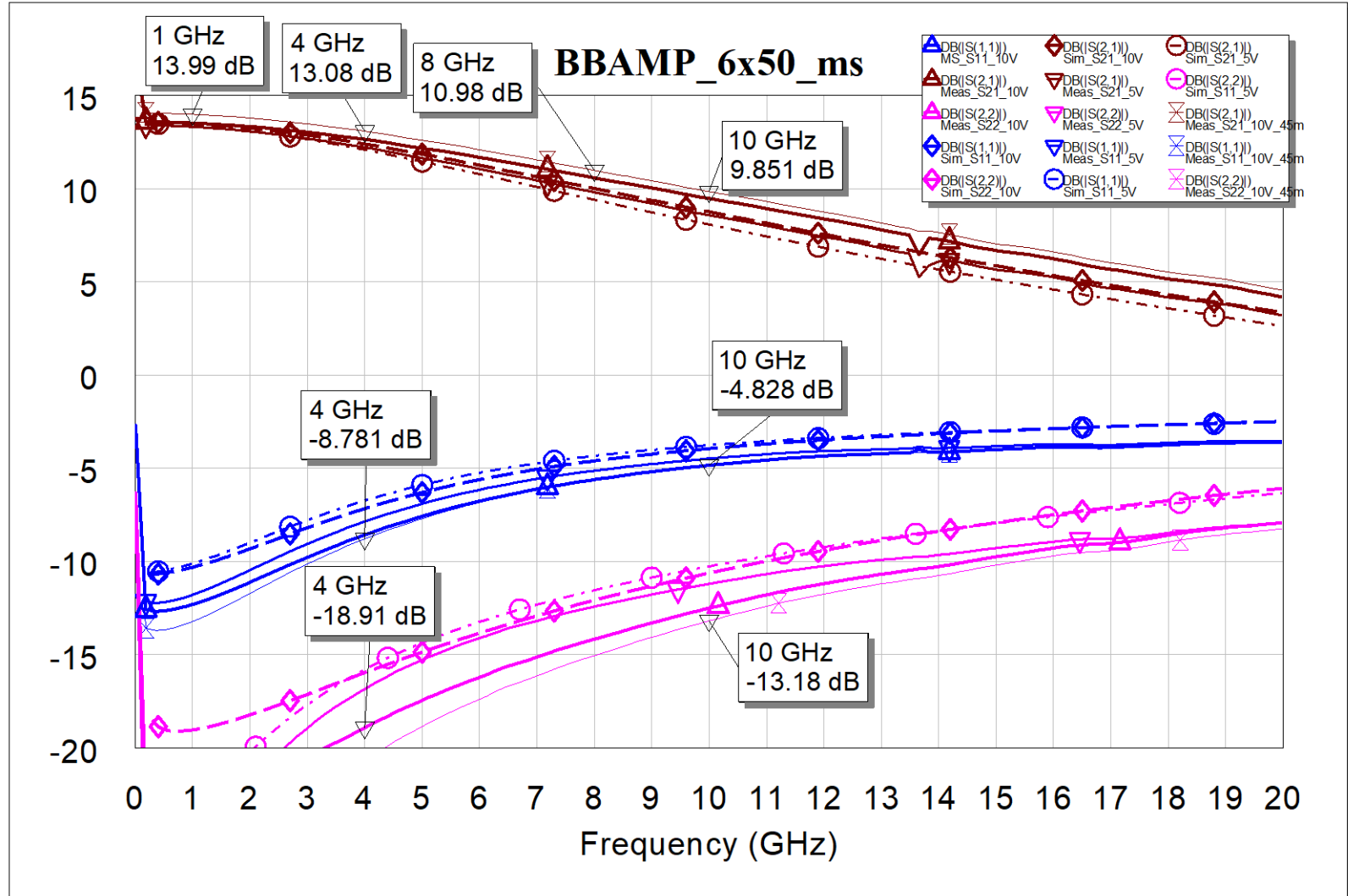


Fig. 18 Measured (solid) vs. simulation (dash) of 6- × 50- $\mu\text{m}$  resistive-feedback amplifier

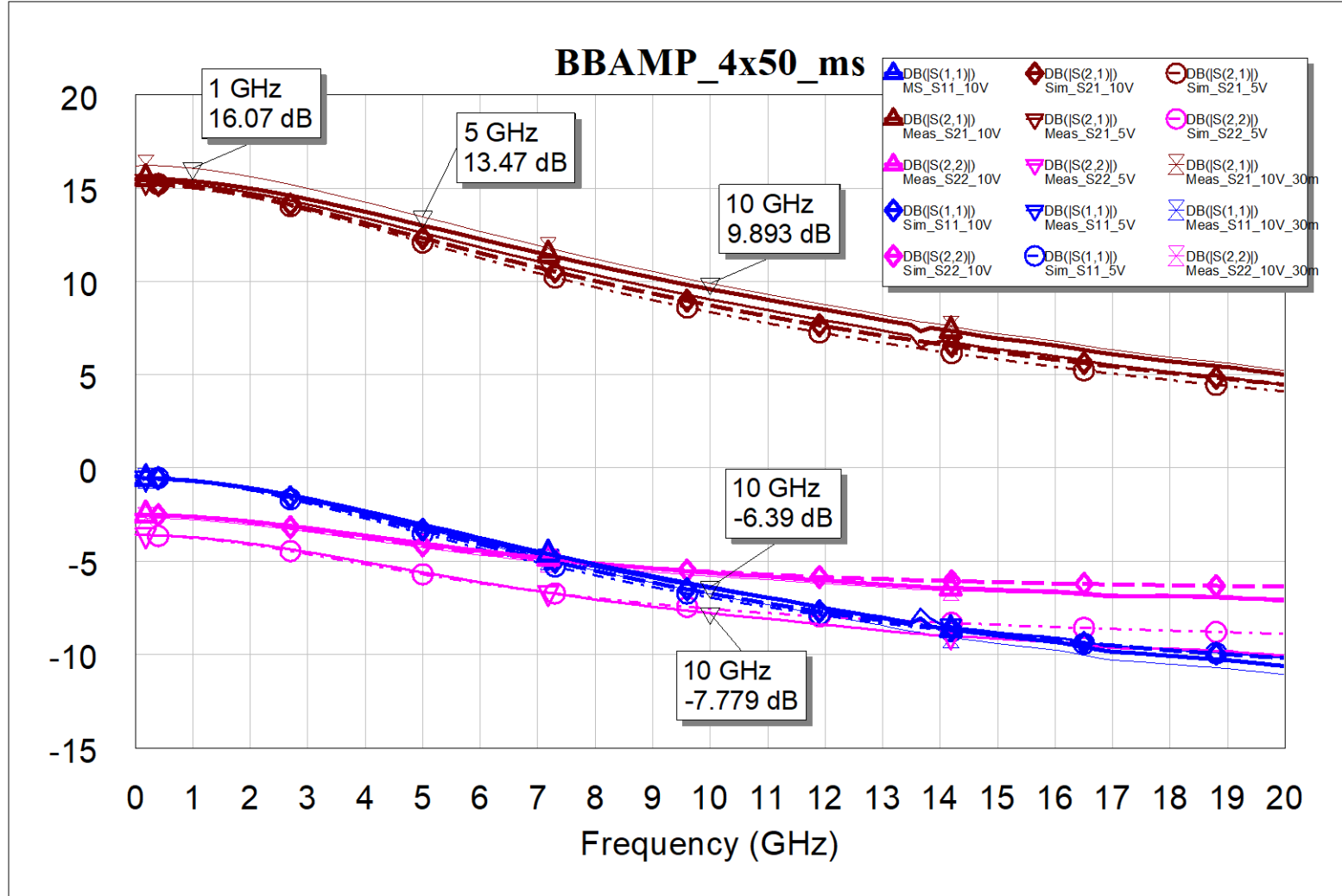


Fig. 19 Measured (solid) vs. simulation (dash) of 4-  $\times$  50- $\mu\text{m}$  source-feedback amplifier (10 V)

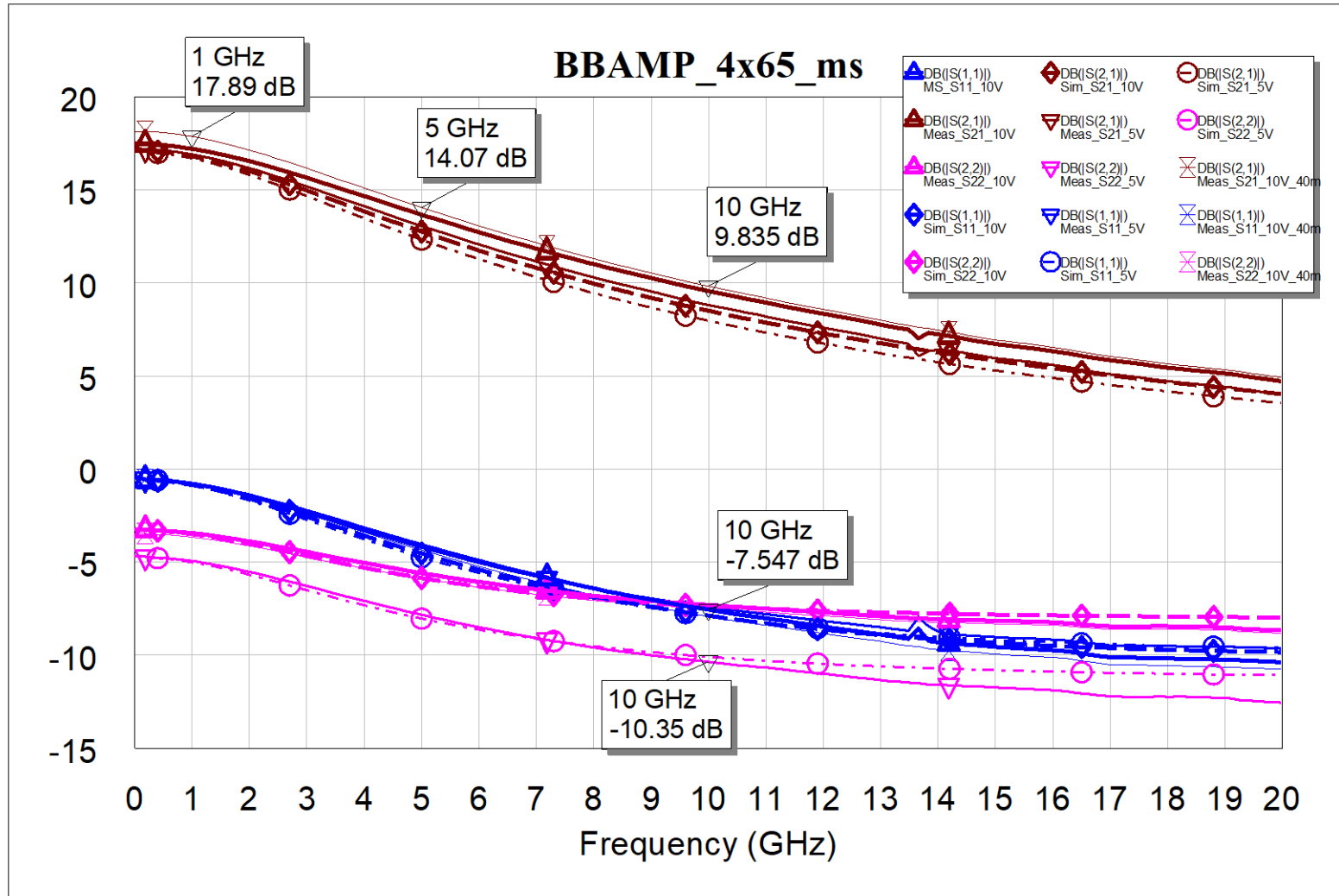


Fig. 20 Measured (solid) vs. simulation (dash) of  $4 \times 65\text{-}\mu\text{m}$  source-feedback amplifier (10 V)

Figure 21 shows output power (blue), PAE (magenta), and gain (brown) measured (solid) versus simulation (dash) in plots of the  $6\text{-} \times 50\text{-}\mu\text{m}$  amplifier, at 10- and 20-V DC bias and at 6 GHz. There is excellent agreement between simulations and measurements with almost 1/2 W of output at 20 V, but better efficiency up to 25% peak PAE at 10 V at a lower 1/3-W output power. Figures 22 and 23 show similar power performance at 8 and 10 GHz with similar output powers of 1/2 W (20 V) and 25% peak PAE (10 V). Given the lower gain at 10 GHz, the output power is not driven into as much compression at the shown measured peak of 26.5 dBm.

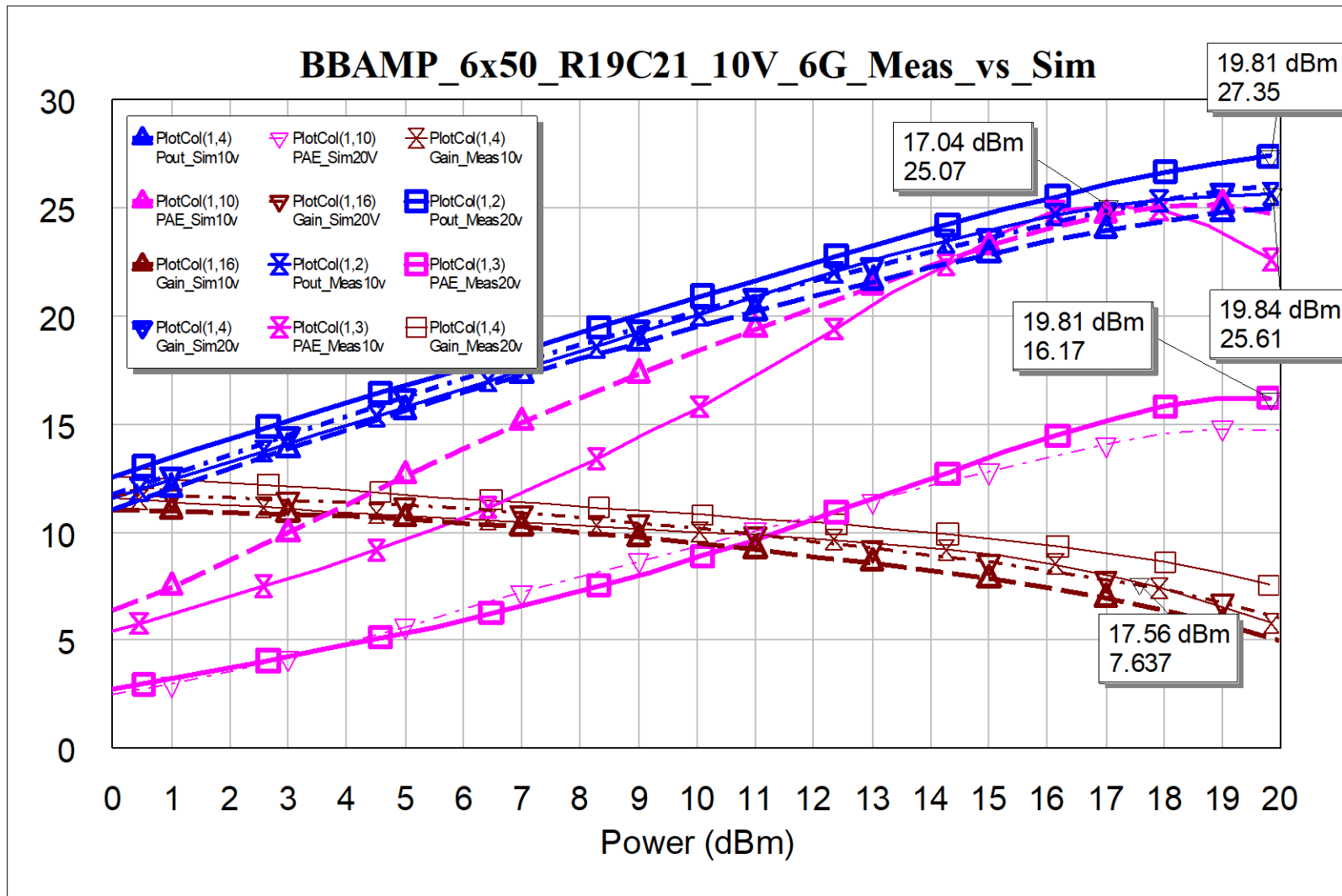


Fig. 21 Measured (solid) vs. simulation (dash) at 6 GHz, 6- × 50- $\mu$ m amplifier (10 and 20 V)

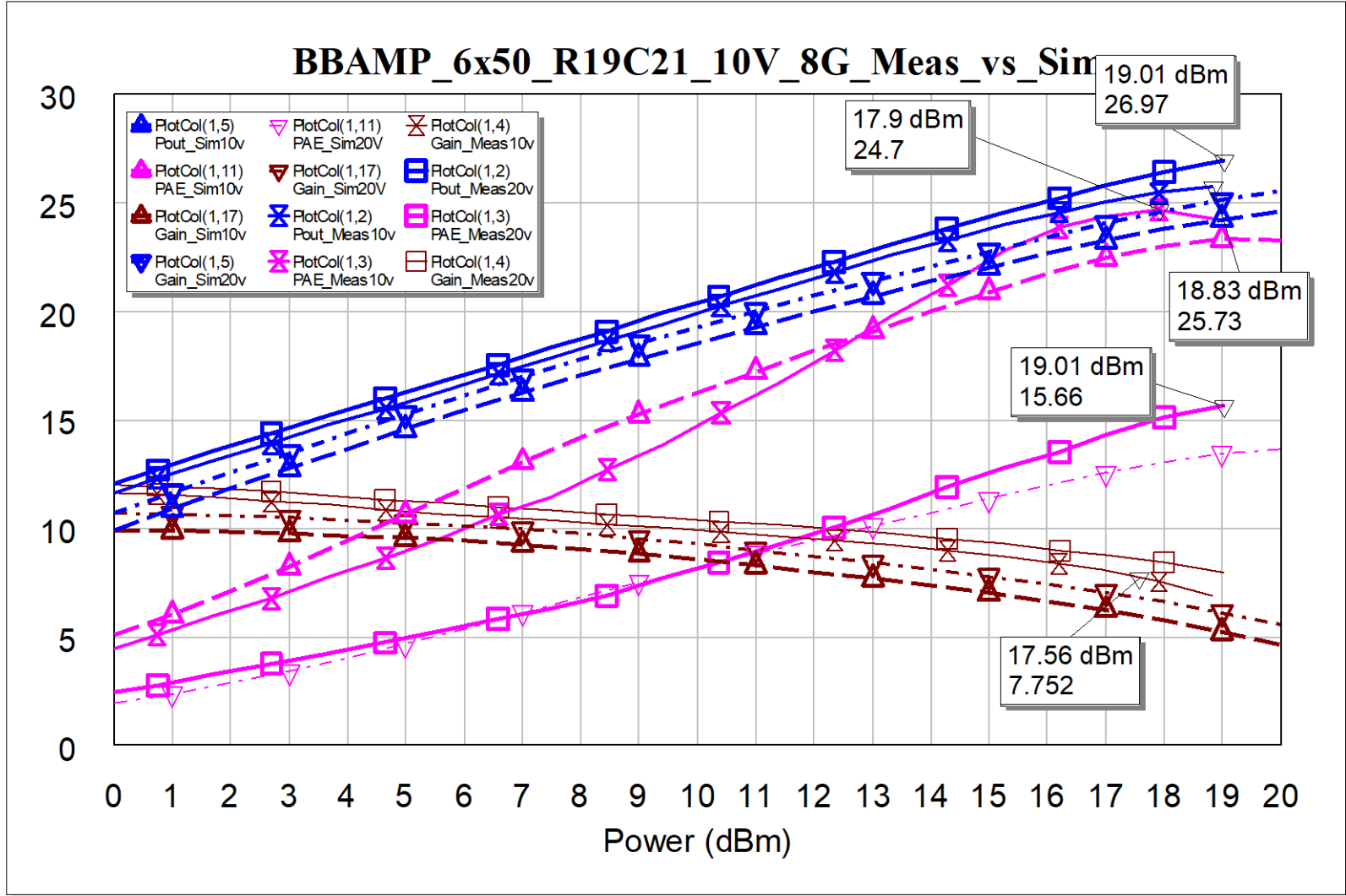


Fig. 22 Measured (solid) vs. simulation (dash) at 8 GHz, 6- × 50- $\mu$ m amplifier (10 and 20 V)

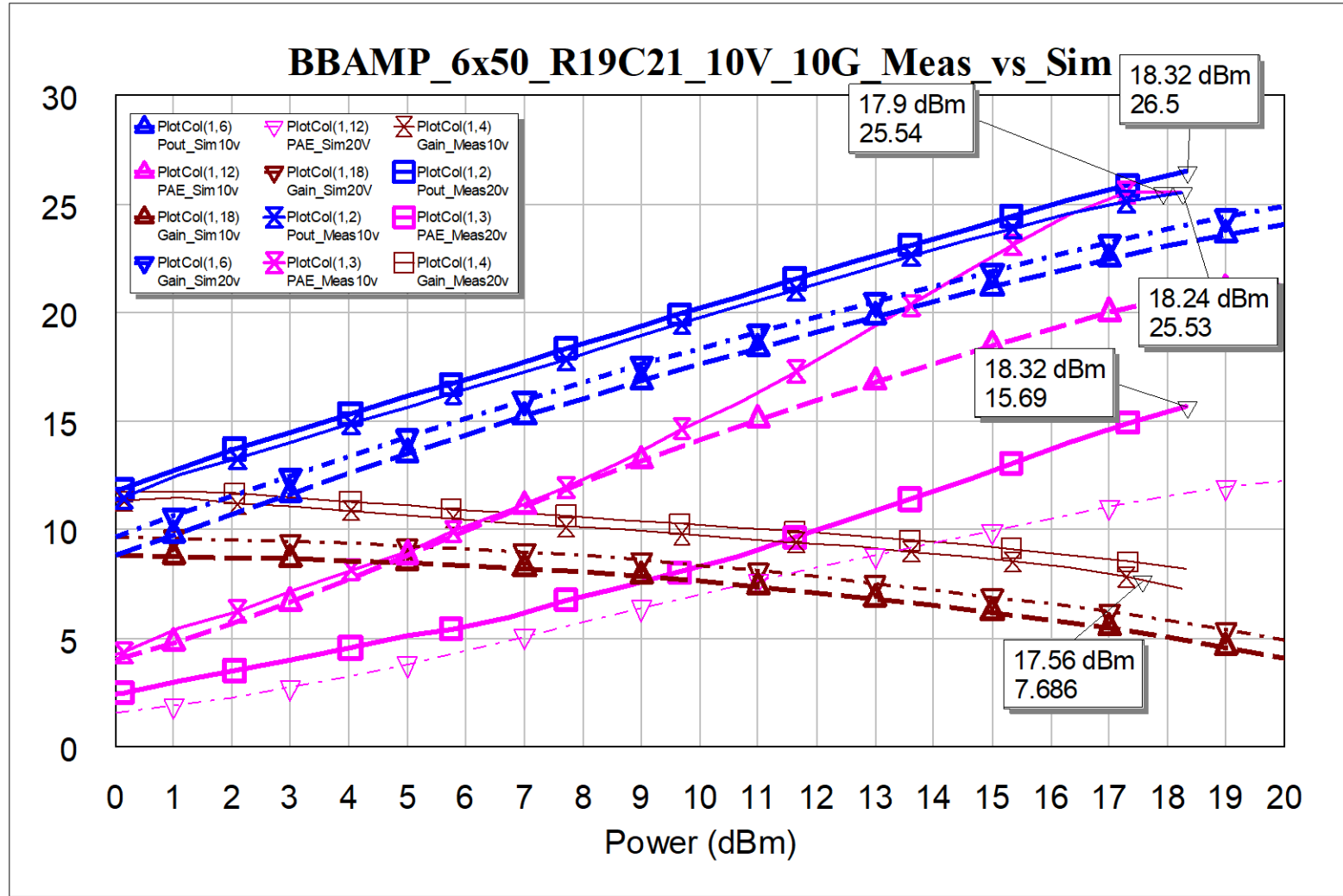


Fig. 23 Measured (solid) vs. simulation (dash) at 10 GHz, 6- $\times$  50- $\mu$ m amplifier (10 and 20 V)

Power performance for the  $4 \times 50\text{-}\mu\text{m}$  source-feedback broadband amplifier is even higher than simulations. Figure 24 shows output power (blue), PAE (magenta), and gain (brown) in measured (solid) versus simulation (dash) plots of the  $4 \times 50\text{-}\mu\text{m}$  amp at 10- and 20-V DC bias and at 6 GHz. There is peak of 0.7 W of output at 20 V and excellent efficiency up to 39% peak PAE at 10 V at a lower 0.3-W output power. Figure 25 shows similar power performance at 8 GHz. With the lower gain at 10 GHz, Fig. 26 shows power performance at 10 GHz, which has not compressed much, yet still yields an output power of 0.55 W (20 V) and 39% peak PAE (10 V) corresponding to nearly 1/2 W of output power.

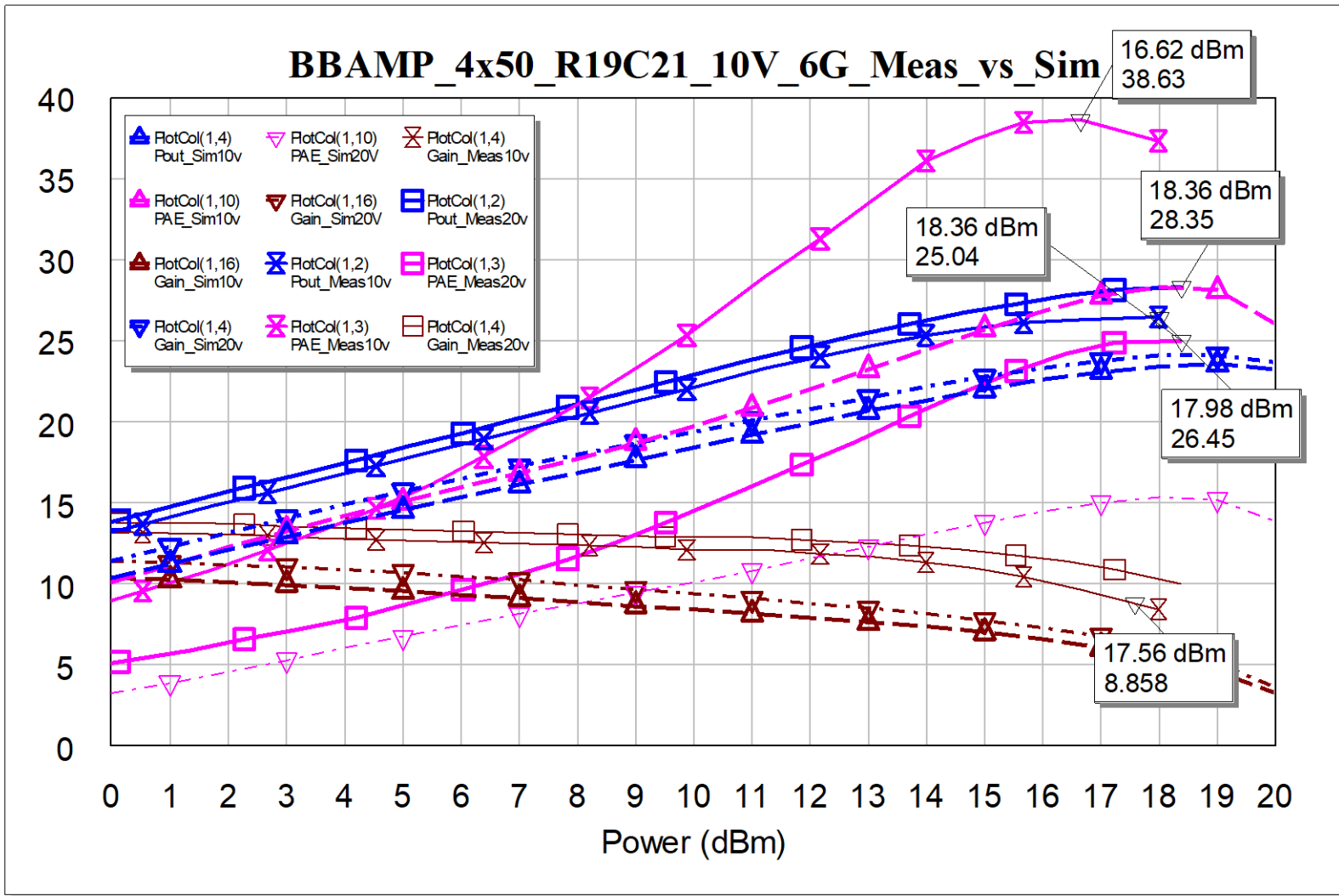


Fig. 24 Measured (solid) vs. simulation (dash) at 6 GHz, 4- × 50- $\mu$ m amplifier (10 and 20 V)

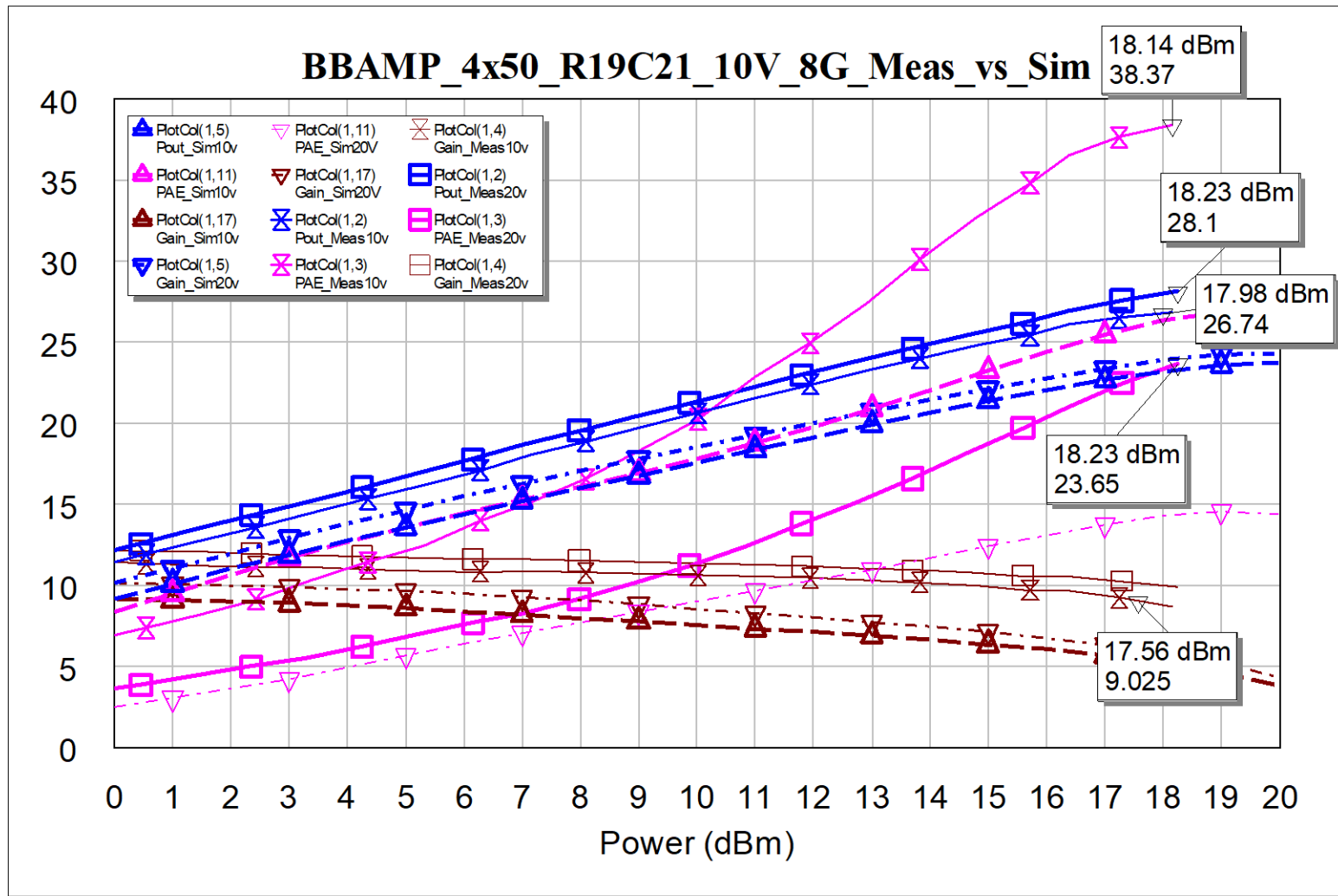


Fig. 25 Measured (solid) vs. simulation (dash) at 8 GHz, 4- × 50- $\mu$ m amplifier (10 and 20 V)

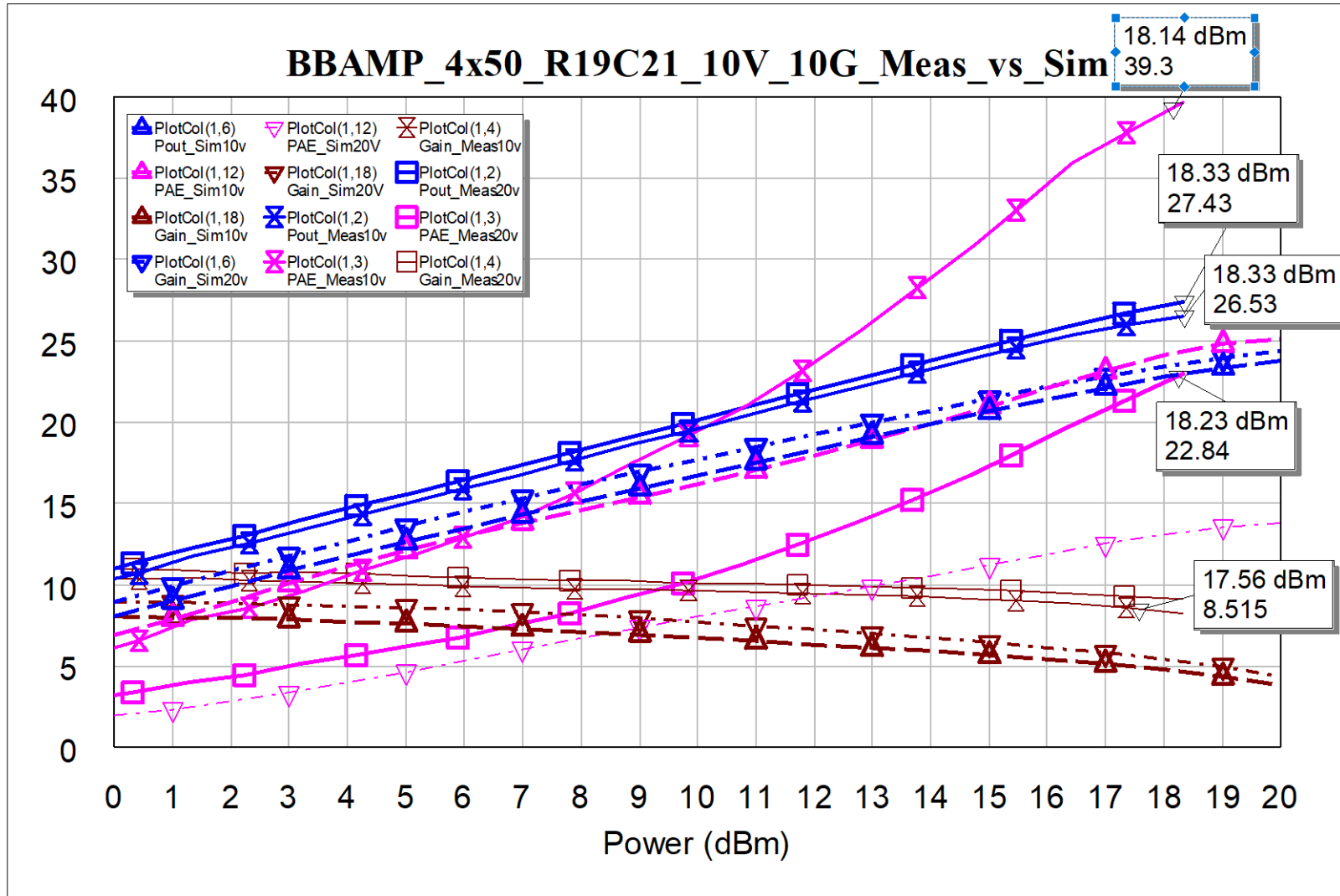


Fig. 26 Measured (solid) vs. simulation (dash) at 10 GHz, 4- × 50- $\mu$ m amplifier (10 and 20 V)

Figure 27 shows power performance for the  $4 \times 65\text{-}\mu\text{m}$  source-feedback broadband amplifier is good but not as high as the prior  $4 \times 50\text{-}\mu\text{m}$  amplifier. Figure 28 shows output power (blue), PAE (magenta), and gain (brown) in measured (solid) versus simulation (dash) plots of the  $4 \times 65\text{-}\mu\text{m}$  amplifier at 10- and 20-V DC bias and at 6 GHz. There is peak of almost 1/2 W of output at 20 V and good efficiency up to 34% peak PAE at 10 V at a lower 0.3-W output power. Figure 29 shows similar power performance at 8 GHz. At 10 GHz, Fig. 30 also shows similar good power performance at 10 V, while the 20-V measurements taken were not available for this report. Performance and efficiency are good as a power amplifier yet it is also expected to have an excellent noise figure. Hopefully, noise figure-measurements can be made in the future.

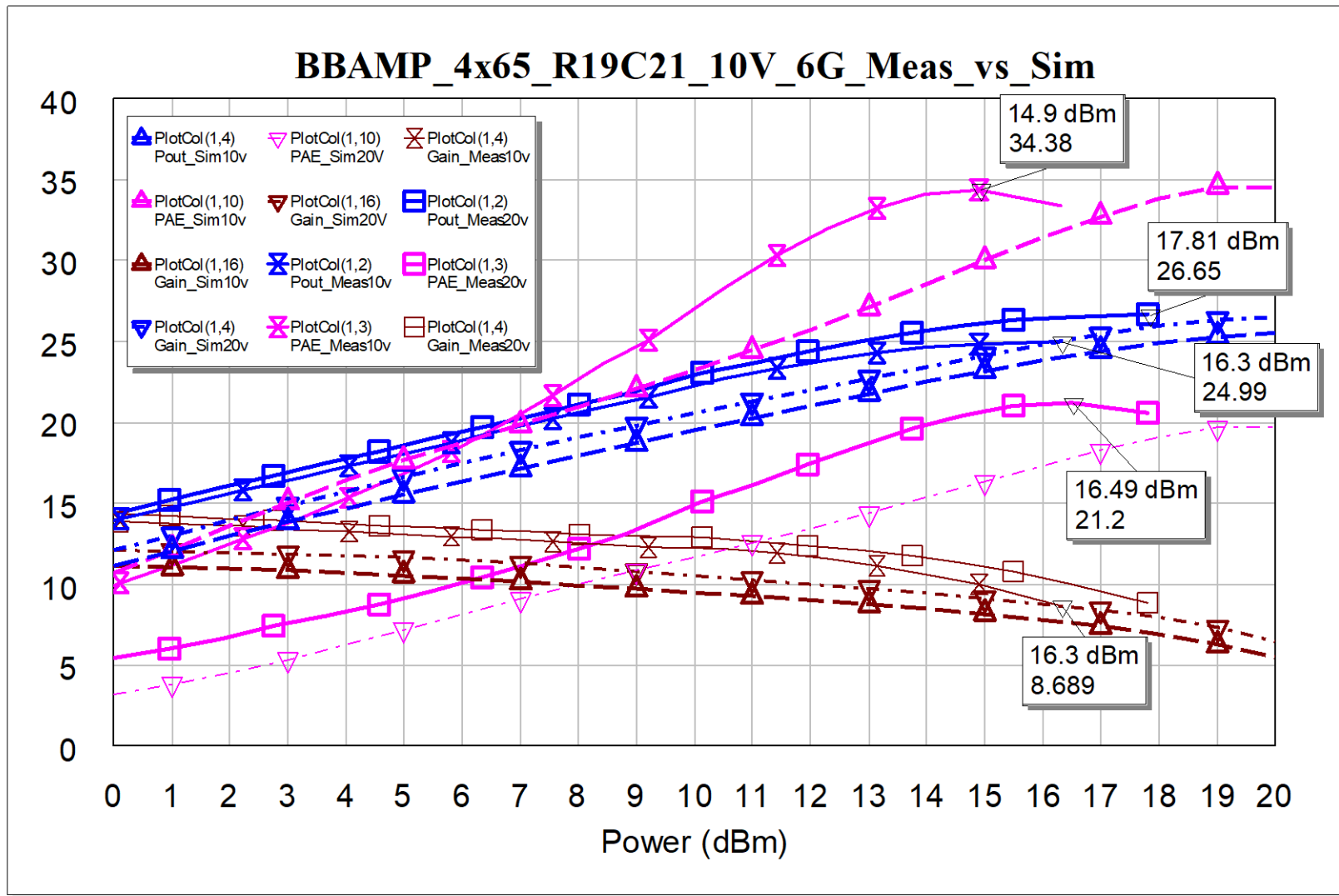


Fig. 27 Measured (solid) vs. simulation (dash) at 6 GHz, 4- × 65-μm amplifier (10 and 20 V)

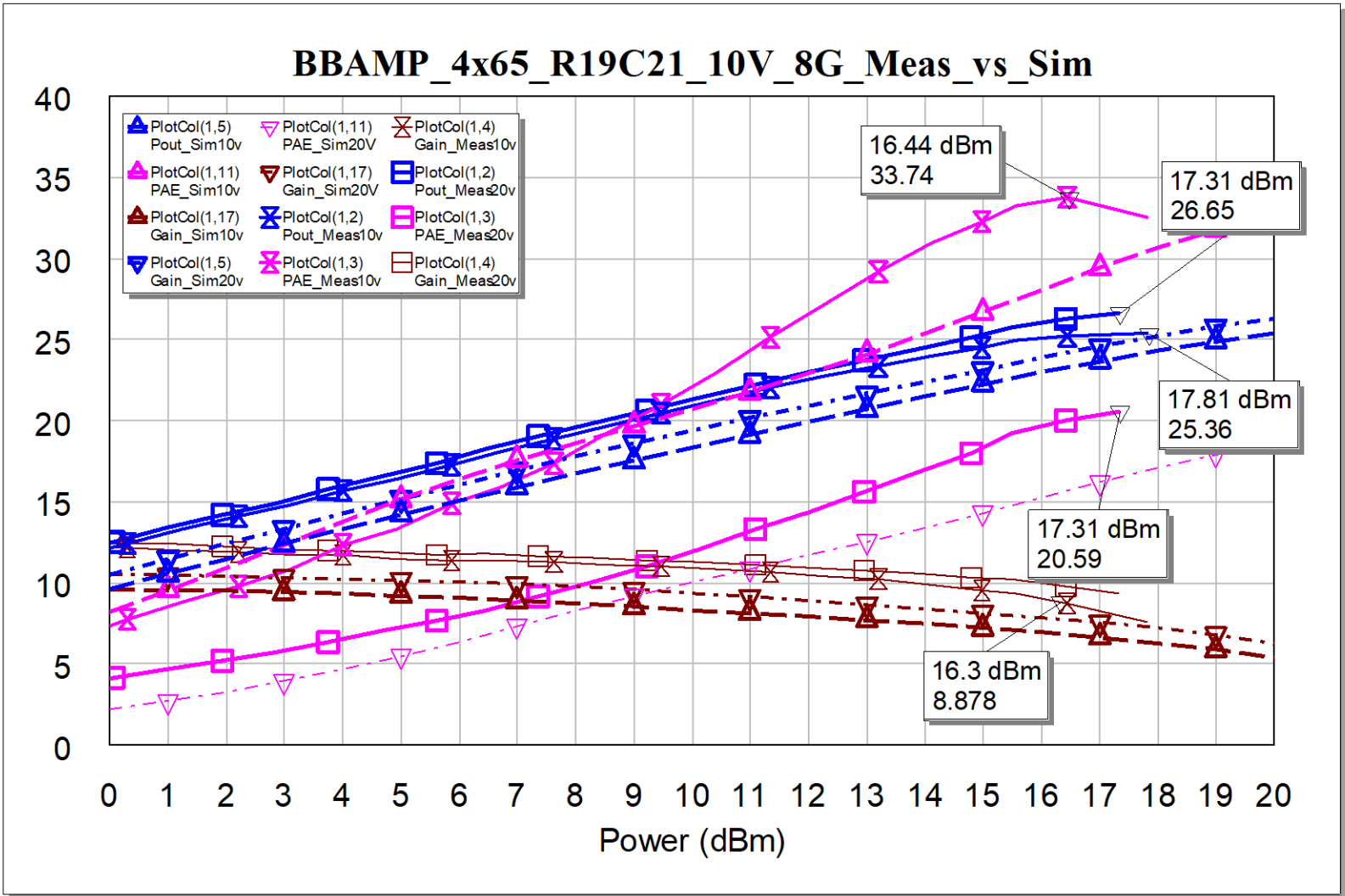


Fig. 28 Measured (solid) vs. simulation (dash) at 8 GHz, 4-  $\times$  65- $\mu\text{m}$  amplifier (10 and 20 V)

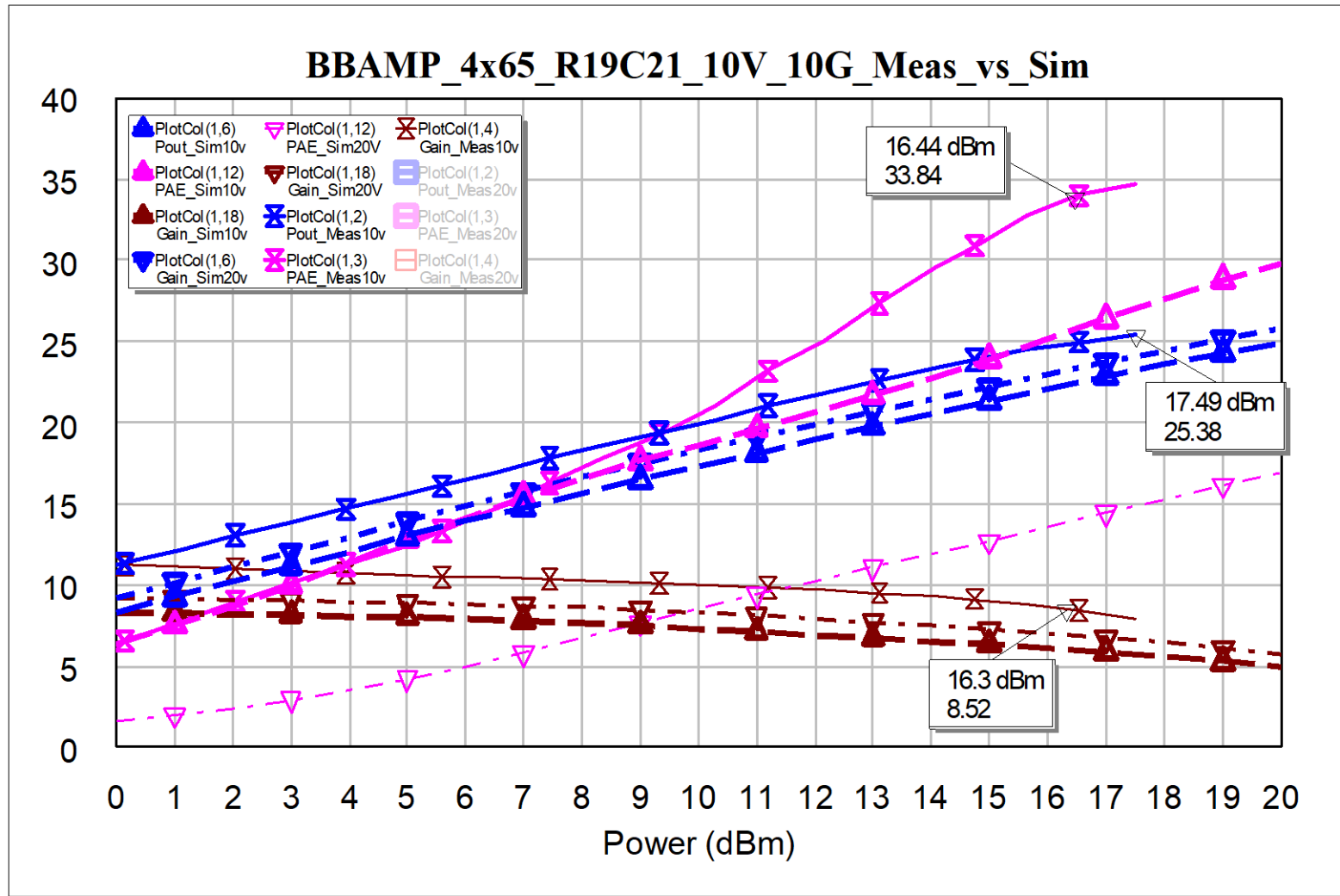
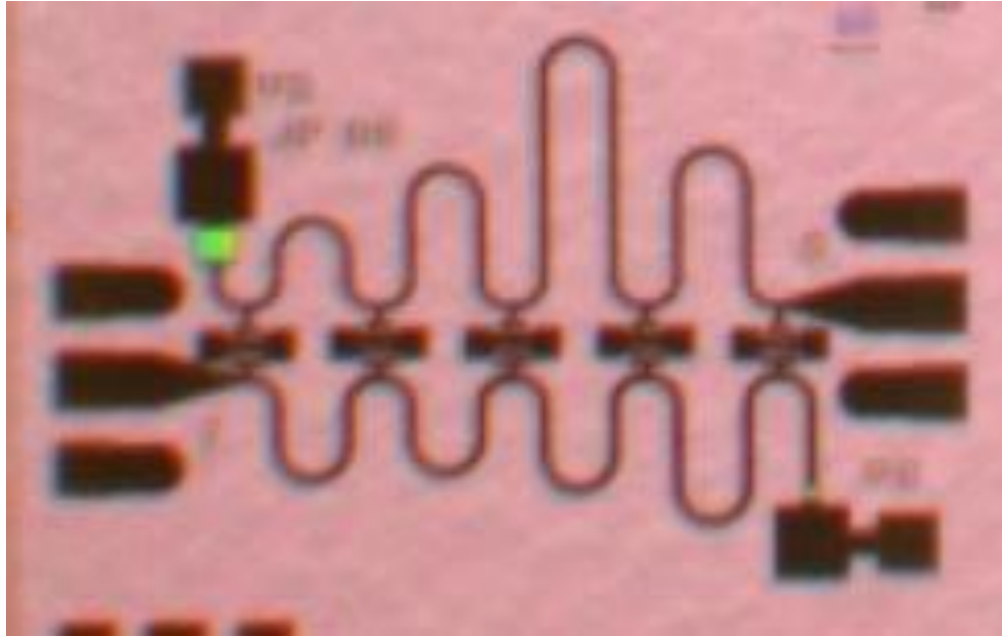


Fig. 29 Measured (solid) vs. simulation (dash) at 10 GHz, 4- × 65- $\mu$ m amplifier (10 and 20 V)



**Fig. 30** Photo of nonuniform distributed amplifier (NUDA),  $1.5 \times 1.0$  mm

## **6. Broadband Nonuniform Distributed Amplifier**

---

Distributed amplifiers (DAs) provide very broadband gain, decades of bandwidth, but typically compromise on power and efficiency or low noise performance. NUDAs have been explored to achieve large bandwidth gain with better efficiencies for power amplifiers. A nonuniform approach was explored, but this design was targeted for lower noise figure. Figure 30 shows a picture of the DA. Figure 31 shows measured (solid) versus simulations (dash) of the NUDA MMIC layout with excellent broadband-gain performance matching well with simulations at 5- and 10-V DC biases. Gain is still near 10 dB from 2 to 28 GHz, falling to about 7 dB gain at 32 GHz. The amplifier can work over a range of DC biases but was intended for low noise, at 5 or 10 V. Measurements at 20 and 28 V show similar gain performance up to about 28 GHz, but the gain rolls off more with increasing drain voltage. This distributed amplifier does not have as much bandwidth as a prior design using a Raytheon 0.14- $\mu\text{m}$  GaN process<sup>2</sup> but operates at a higher voltage, which would typically result in higher dynamic range. Compared with another recent distributed amplifier in Qorvo 0.25- $\mu\text{m}$  GaN process,<sup>3</sup> this amplifier has higher bandwidth but potentially less dynamic range than the longer 0.25- $\mu\text{m}$  gate length design.

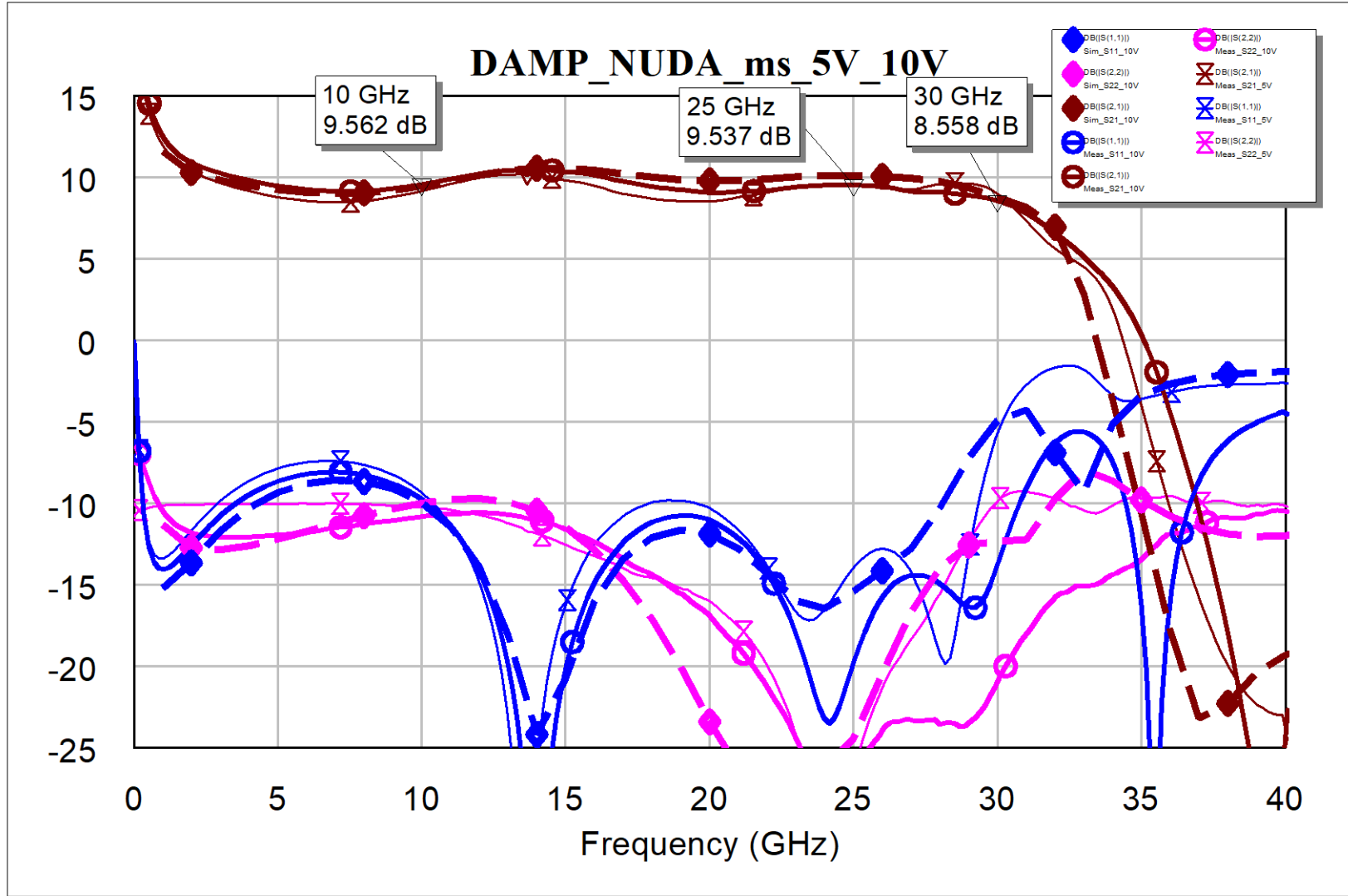


Fig. 31 Measured (solid) vs. simulation (dash) of NUDA (10 V)

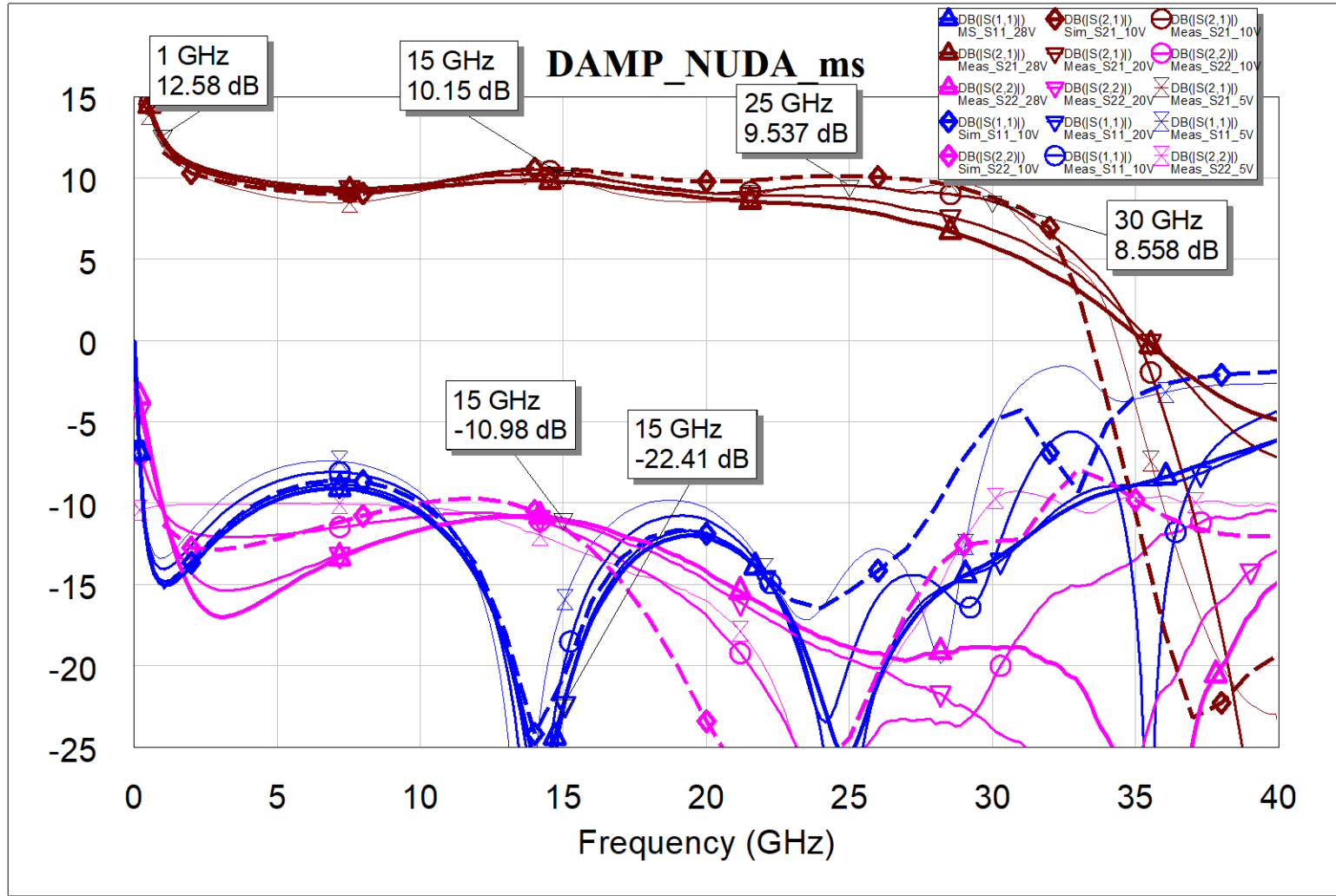


Fig. 32 Measured (solid) vs. simulation (dash) of NUDA (20 V)

## 7. Other Broadband-Amplifier Test Circuits

---

There were a couple of experimental circuits that demonstrated broadband performance. Dr Ali Darwish had an interesting idea: Take a design for a different process, such as 0.25- $\mu\text{m}$  GaN, swap the HEMTs, and it might work reasonably well. A couple of experimental circuits did just that, by swapping the original HEMT devices with HEMTs from this 0.15- $\mu\text{m}$  GAN15\_ES process. While not designed to be optimal, there was room on the entire wafer run to try out this experiment and test Dr Darwish's idea.

A cascode HEMT arrangement should yield more gain bandwidth than a typical grounded-source HEMT. Previously, a cascode DA was designed for Qorvo's 90-nm high-performance "research" (i.e., prerelease) GaN process. Layout of the cascode HEMTs is complicated, but for this test a new cascode DA design was quickly created using 0.15- $\mu\text{m}$  HEMTs to swap out HEMTs from a prior 90-nm design. The gain performance was predicted to be greater than the common-source NUDA design previously discussed. Stability is also more complicated, given the increased gain bandwidth. Testing requires careful application of the DC biases, drain, and two gate voltages to split the supply across the cascode HEMT pairs.

Figure 33 shows a picture of the cascode DA. Figure 34 shows measured (solid) versus simulations (dash) of the cascode MMIC layout with enhanced broadband-gain performance, but with an unexpected ripple. Further redesign could flatten out the gain with some additional analysis. It certainly demonstrates the potential for an increased gain bandwidth using a cascode arrangement.

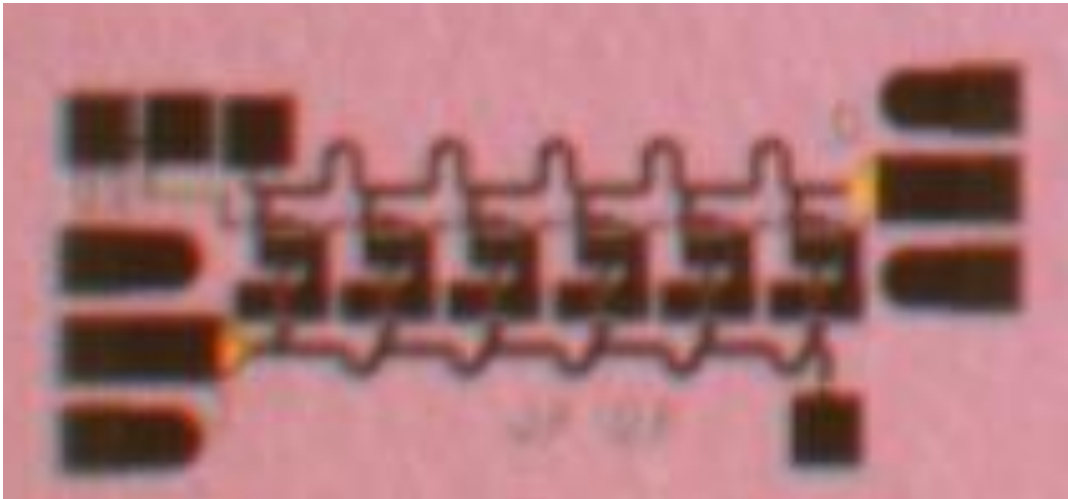


**Fig. 33** Photo of cascode DA (1.3  $\times$  0.6 mm)

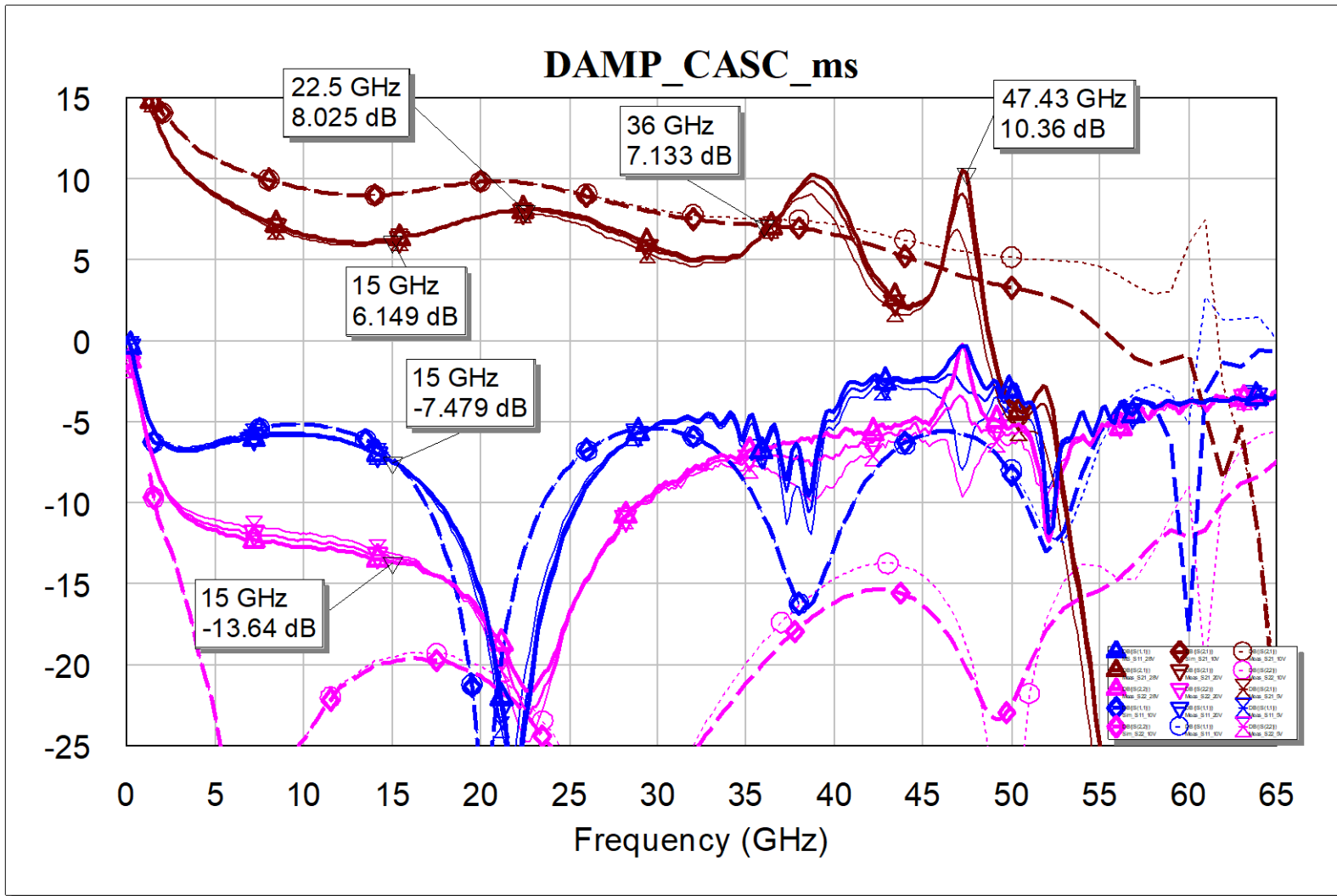


Fig. 34 Measured (solid) vs. simulation (dash) of cascode DA (20 V)

Another feedback amplifier used a design that was previously done in 0.25- $\mu\text{m}$  GaN, so the HEMT was replaced with a 0.15- $\mu\text{m}$  HEMT. The expectation would be for similar broadband performance with slightly more gain in the new design. Figure 35 shows a picture of the very small broadband 4-  $\times$  110- $\mu\text{m}$  feedback amplifier. Figure 36 shows measured (solid) versus simulations (dash) of the 4-  $\times$  110- $\mu\text{m}$  feedback MMIC layout.



**Fig. 35** Photo of 4-  $\times$  110- $\mu\text{m}$  feedback broadband amplifier (0.5  $\times$  0.6 mm)

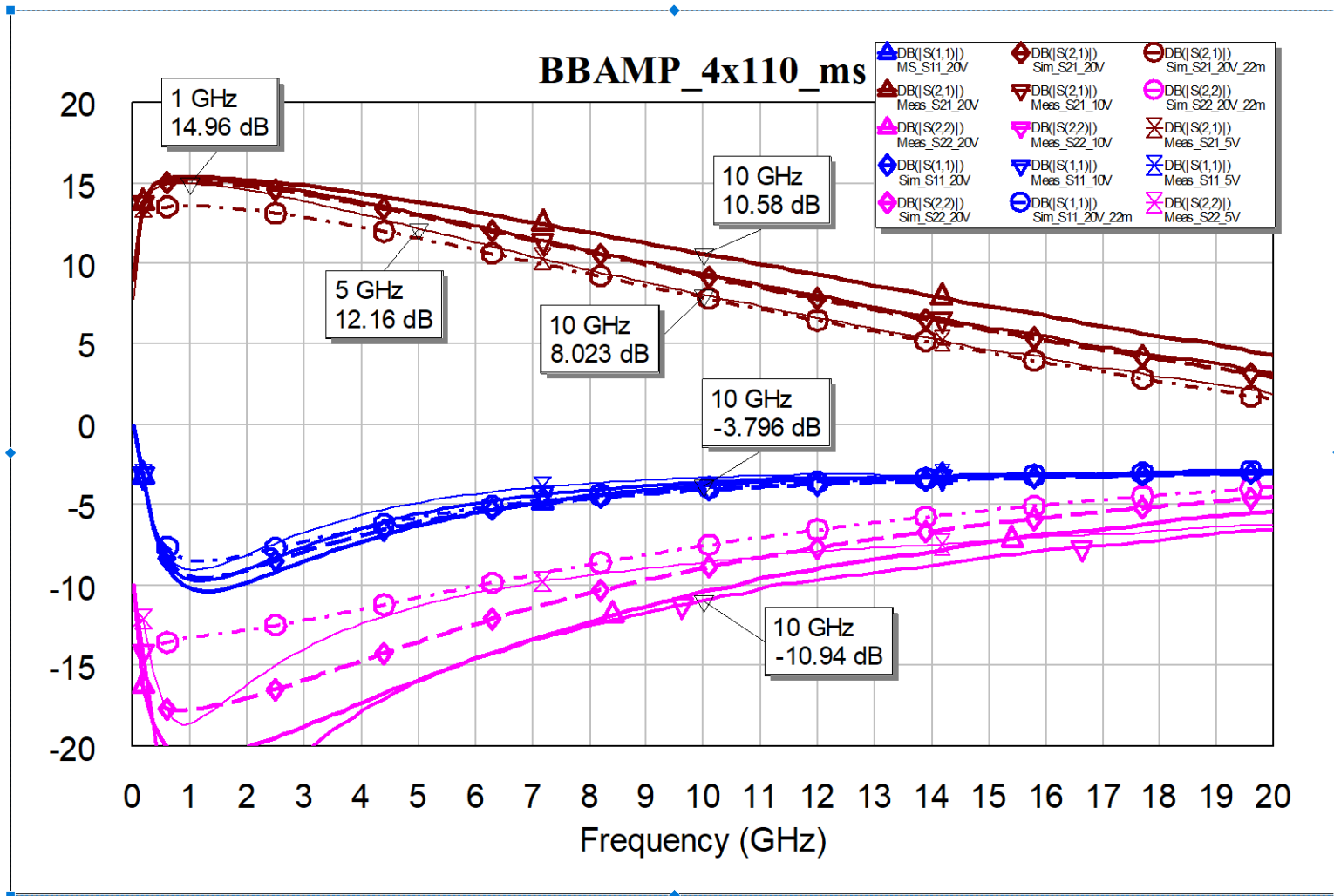


Fig. 36 Measured (solid) vs. simulation (dash) of  $4 \times 110\text{-}\mu\text{m}$  feedback amplifier (10, 20 V)

Even though the design was originally for a 0.25- $\mu\text{m}$  GAN process, power performance for the 4-  $\times$  110- $\mu\text{m}$  feedback broadband amplifier was very good. Figure 37 shows output power (blue), PAE (magenta), and gain (brown) in measured (solid) versus simulation (dash) plots of the 4-  $\times$  110- $\mu\text{m}$  amplifier at 10- and 20-V DC bias for 6 GHz. There is peak of 0.75 W of output at 20 V and good efficiency up to 31% peak PAE at 10 V at a lower 0.5-W output power. Figure 38 shows similar power performance at 8 GHz, but was not driven to the same compression levels as at 6 GHz. At 10 GHz, Fig. 39 also shows similar good power performance with a peak of almost 0.7 W and 20% PAE at 20 V and almost 1/2 W and 31% PAE at 10 V. This design worked very well as a broadband amplifier with good gain and efficiency.

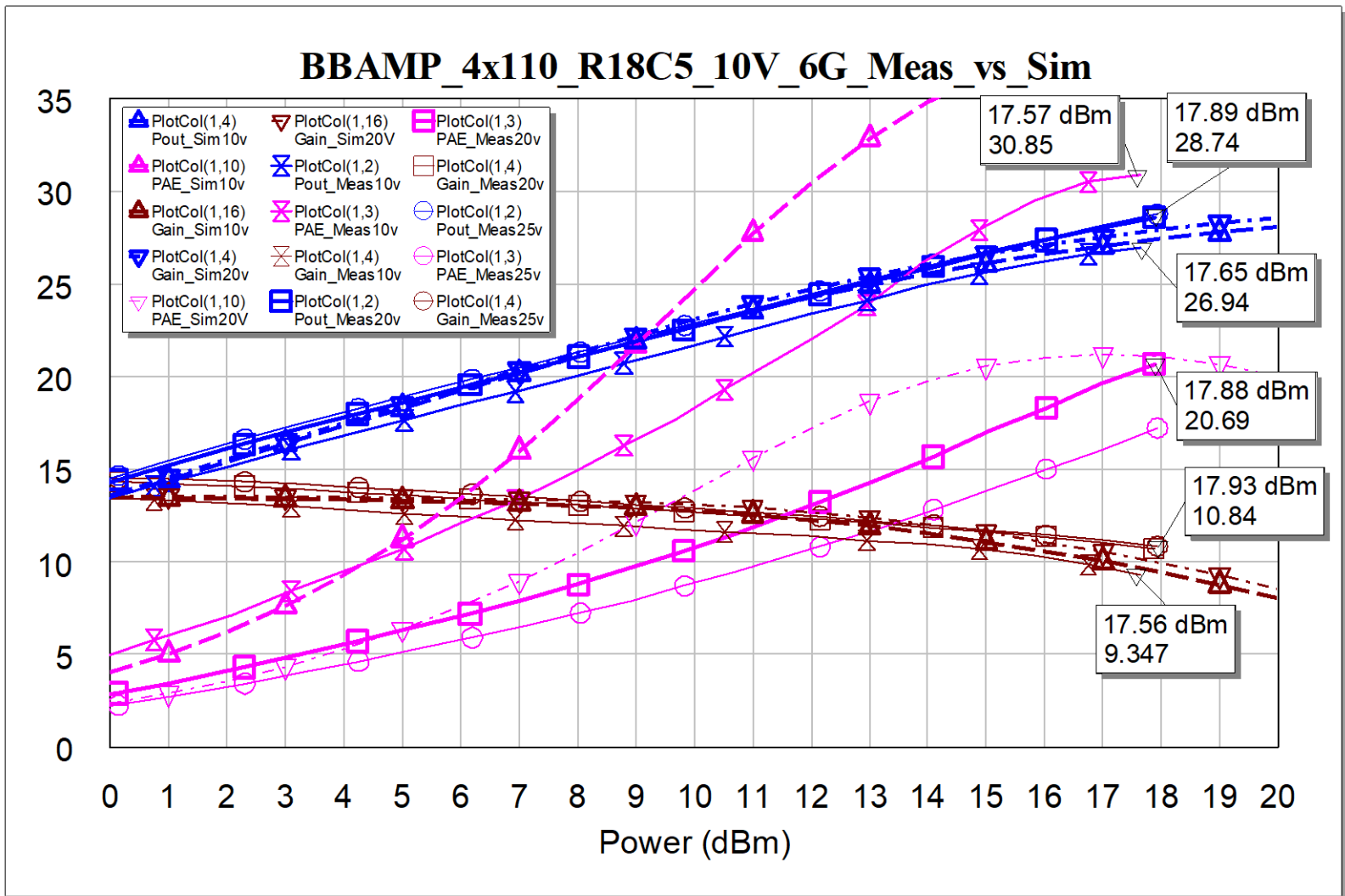


Fig. 37 Measured (solid) vs. simulation (dash) at 6 GHz, 4- × 110-μm amplifier (10 and 20 V)

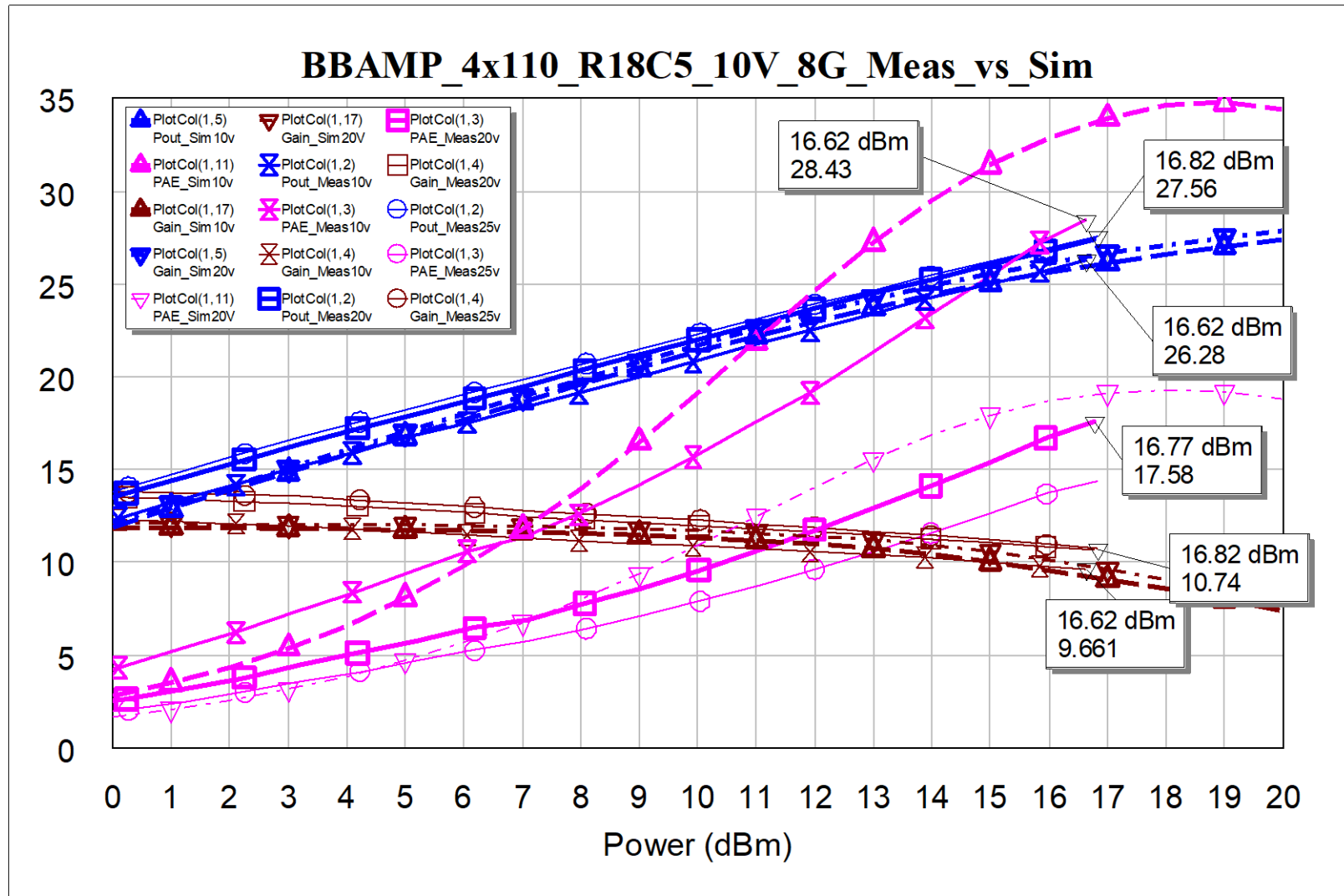


Fig. 38 Measured (solid) vs. simulation (dash) at 8 GHz, 4- × 110-μm amplifier (10 and 20 V)

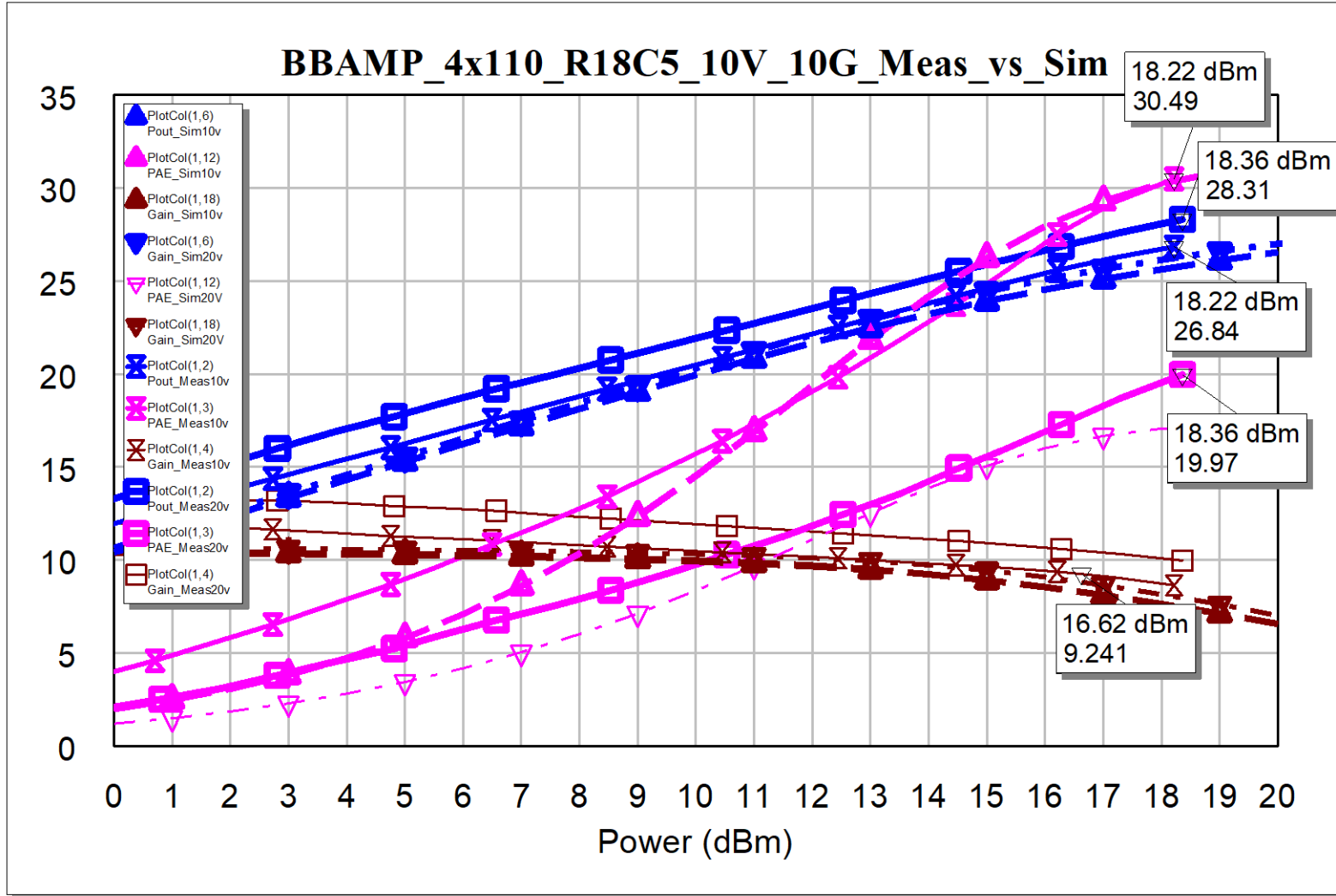


Fig. 39 Measured (solid) vs. simulation (dash) at 10 GHz, 4- × 110-μm amplifier (10 and 20 V)

## 8. Conclusions

---

Multiple MMIC designs were submitted to an ARL Qorvo 0.15- $\mu\text{m}$  GaN Prototype Wafer Option to demonstrate the performance, bandwidth, capability, versatility, and applicability of GaN for compact, efficient, microwave circuit designs, particularly for air and missile defense radars but also for EW, network communications, and efficient amplifiers for future radio and communications networks.<sup>4</sup>

Almost all of the die tested worked the first time, implying excellent yield for the Qorvo 0.15- $\mu\text{m}$  GaN process. Most of the measurements agree quite well with the expected simulations. Some models are more accurate than others, depending on device size, application (e.g., switch vs. amplifier), frequency, DC bias, and so on. At this time, because of the national health crisis, noise measurements could not be performed but should be done in follow-up. Testing such small high-power amplifiers must be done carefully, verifying stability before performing tests so as not to damage equipment or, in some cases, not to test PAs beyond 10 W at the die level due to probe limits. In a few cases, power performance needs to be tested further at higher frequencies, using load pull to verify the accuracy of the nonlinear models and of these designs. Lessons learned could be applied to improve performance in a future redesign or, with some clever package designs, to enhance the current performance.

The III/V MMIC team has designed a number of creative, high-performance circuits from a recent wafer fabrication in Qorvo's 0.15- $\mu\text{m}$  commercial GAN process<sup>5</sup> that recently have been tested (or should be soon) and documented. Some of these designs will be packaged for further demonstrations and applications.

## 9. References

---

1. Penn J. Low-noise amplifiers (LNAs) and power amplifiers (PAs) for next-generation S- and X-band radars. Aberdeen Proving Ground (MD): CCDC Army Research Laboratory (US); 2019 Dec. Report No.: ARL-TR-8871.
2. Penn JE, Darwish A. Broadband low noise gallium nitride (GaN) amplifiers for next generation radars. Aberdeen Proving Ground (MD): Army Research Laboratory (US); 2017 Nov. Report No.: ARL-TR-8208.
3. Penn J. Testing of 0.25- $\mu\text{m}$  gallium nitride (GaN) monolithic microwave integrated circuit (MMIC) designs. Aberdeen Proving Ground (MD): Army Research Laboratory (US); 2018 Nov. Report No.: ARL-TR-8565.
4. Penn J, Darwish A, Hawasli S, McKnight K. Gallium nitride high-electron-mobility transistor (HEMT) monolithic microwave integrated circuit (MMIC) designs submitted for Qorvo prototype wafer option (PWO) fabrication. Aberdeen Proving Ground (MD): CCDC Army Research Laboratory (US); 2019 Nov. Report No.: ARL-TR-8811.
5. Penn J, Darwish A. Ka-band front-end monolithic microwave integrated circuits (MMICs) and transmit–receive (T/R) modules testing. Aberdeen Proving Ground (MD): CCDC Army Research Laboratory (US); 2020 Apr. Report No.: ARL-TR-8940.

## List of Symbols, Abbreviations, and Acronyms

---

ARL	US Army Research Laboratory
CCDC	US Army Combat Capabilities Development Command
DA	distributed amplifier
DC	direct current
EM	electromagnetic
GaN	gallium nitride
HEMT	high electron mobility transistor
$I_{DS}$	drain current
LNA	low-noise amplifier
MMIC	monolithic microwave integrated circuit
NUDA	nonuniform distributed amplifier
PA	power amplifier
PAE	power-added efficiency

1 DEFENSE TECHNICAL  
(PDF) INFORMATION CTR  
DTIC OCA

1 CCDC ARL  
(PDF) FCDD RLD CL  
TECH LIB

11 CCDC ARL  
(PDF) FCDD RLS R  
1 P AMIRTHARAJ  
(HC) FCDD RLS RE  
R DEL ROSARIO  
A DARWISH  
T IVANOV  
P GADFORT  
S HAWASLI  
K KINGKEO  
K MCKNIGHT  
J PENN (1 HC)  
E VIVEIROS  
J WILSON